Technische Universität München

Fakultät für Medizin

Investigating the role of BET bromodomain proteins for Ewing Sarcoma specific expression profiles and malignancy

Fiona Becker-Dettling

Fakultät für Medizin der Technischen Universität München

Kinderklinik der Technischen Universität München, Labor für Funktionelle Genomik und Transplantationsbiologie, Children's Cancer Research Center Munich

Investigating the role of BET bromodomain proteins

for Ewing sarcoma specific expression profiles and malignancy

Fiona Anni Gerda Becker-Dettling

Vollständiger Abdruck der von der Fakultät für Medizin der Technischen Universität München zur Erlangung des akademischen Grades eines Doktors der Medizin genehmigten Dissertation.

Vorsitzende: Prof. Dr. Jürgen Schlegel

Prüfer der Dissertation:

1. Priv.-Doz. Dr. Günther Richter
2. Priv.-Doz. Dr. Katja Specht

Die Dissertation wurde am 16.10.2019 bei der Technischen Universität München eingereicht und durch die Fakultät für Medizin am 07.04.2020 angenommen.

Acknowledgments

Firstly, I would like to express my sincere gratitude to my supervisor **PD Dr. rer. nat. Richter** for his strong and continuous support, his motivation and immense knowledge – Günther, your guidance and understanding helped me in all the time of research and writing of this thesis. I could not have imagined having a better mentor.

Additionally, I would like to thank my lab adviser **Dr. rer. nat. Hensel** for his cooperation, his patience and insightful comments and my fellow lab family members Isabel, David, Andi, Oxana and Kristina for their excellent team spirit.

Finally, my thanks go to the “Children Cancer Research Center Schwabing” and the “Kinderklinik Schwabing” for the access to the laboratory and research facilities to conduct this thesis.

Munich, September 2019

Table of contents

1 INTRODUCTION

1.1 Ewing Sarcoma (EwS)

EwS are highly malignant bone or soft tissue tumors (Richter et al., 2009) that play a key role as a prototypic pediatric bone tumor. A first description made by eponym James Ewing (1866–1943) showed, that this malignancy appeared differently from the formerly well-known osteogenic sarcoma or myeloma (Ewing, 1972). Nowadays this neoplasm represents the second most common bone cancer during childhood and adolescence with a rather stable incidence of 2,93 cases/1.000.000 and a slight predominance for males (Maygarden et al., 1993); (Esiashvili et al., 2008). While most patients are affected at the ages of 10 – 20 years with a peak at the age of 15, the sites of appearance are mostly the long hollow bones and the pelvis. Commonly, non-specific symptoms such as local swelling, variable bone pain, feasible palpable masses or emerging pathological fractures occur during etiopathology, which are often mistaken for signs of growth or injury (Flores et al., 2016). Systemic consequences as intermitting fever or anemia may be present. Histologic radiography depicts an aggressive tumor characterized by a permeative ("moth-eaten") pattern with periosteal involvement and a soft tissue component (Arkader et al., 2013). Patients often have to bear early hematologic metastasis which primarily crop up in the lungs or other bones (Khanna et al., 2017; Richter et al., 2009; von Heyking et al., 2017). EwS are highly aggressive sarcomas and demand a multimodal approach fighting against local and systemic disease: Currently patients undergo standard treatment options including chemotherapy, surgery and radiation or stem cell transplantation (Burdach et al., 2010; Gaspar et al., 2015). Although their prognosis has improved over the last years and various potential approaches including molecular targeted therapy or via transgenic T-cells (TC) supported immunotherapies are now available, treatment of EwS is nonetheless challenging (Thiel et al., 2017). The survival rate, especially in the case of growing metastases or recurrence, still persists intolerably low (Valdes et al., 2017; Yu et al., 2017): 50**%** survival over 3 years in the case of single lung metastases and 10**%** survival over 10 years for patients with osseous metastases (Burdach et al., 2010).

Histologically, EwS belong together with peripheral neuroepithelioma/neuroectodermal tumors (PNET) and Askins Tumors to the Ewing sarcoma family of tumors (ESFT) (Khoury, 2005). The ESFT builds a cluster of small, round, blue cell tumors. The morphologically heterogeneous cancers are merged based on genetic and clinicopathological similarities (Verma et al., 2017). While the origin of EwS cancer cells is still a controversial discussion, there is ample evidence of its derive from a mesenchymal stem cell (MSC) origin (Suva et al., 2009; Tirode et al., 2007). The common ground of the ESFT arises from typical chromosomal translocations, above all involving the *ESR1* (Ewing sarcoma breakpoint region 1) gene on chromosome 22 and variable transcription factors of the ETS family (Delattre et al., 1994; Gamberi et al., 2011). 85% of all cases result in the rearrangement of t(11;22)(q24;q12) creating the EWS-FLI1 fusion protein, followed by 5-10% involving the EWS-ERG (22q12) fusion protein (S. Burdach & H. Jürgens, 2000). These new chimeric products are the main oncogenic drivers which regulate the tumorigenic potential of EwS. A plethora of different transcriptional programs is affected either by gene activation or repression (Riggi et al., 2014; Riggi & Stamenkovic, 2007). EWS-FLI1 acts as an aberrant transcription factor altering the target specificity and inducing a dispositive genomic landscape pattern, a modified gene expression and a metabolic dysregulation (Kovar, 2014; Tanner et al., 2017). Therefore, it represents an attractive therapeutical target in EwS. The EWS-FLI1 fundamental functions in tumorigenesis are mainly to provide proliferation, survival and invasiveness (Grunewald et al., 2012; Grunewald et al., 2013) and to restrain cell differentiation by processing apoptosis or cell cycle arrest (Dauphinot et al., 2001; Garcia-Aragoncillo et al., 2008; Javaheri et al., 2016).

Yet direct inhibition has been tough, the EWS-FLI1 transcriptional mediators or downstream located pathways have been taken into consideration for targeted therapy (Goss & Gordon, 2016; Hensel et al., 2016; Lessnick & Ladanyi, 2012; Ng et al., 2010; Yu et al., 2017). EWS-FLI1 is involved in chromatin regulation concerning epigenetic writers and erasers of transcriptional marks (McCabe et al., 2012). Further epigenomic mapping displayed enhancer and promoter remodeling after downregulation of EWS-FLI1 (Riggi et al., 2014; Tomazou et al., 2015). Anyhow, it is still not sufficiently investigated how EWS-FLI1 modifies the chromatin

states but all in all the findings suggest attacking the resulting specific transcriptional program as a promising therapy completion.

1.2 Epigenetic readers and the BET family

1.2.1 Epigenetics

In the 1950s, the discovery of the DNA initiated a new era in medical research. The knowledge of genetic inheritance, altered genotypes and mutations enabled a pioneer approach against diseases and delivered innovative opportunities regarding cancer treatment. The term *epigenetics* includes the Greek prefix epi- (= over, outside of, around) which implies features lying “above” alterations of the DNA sequence. Epigenetic modifications build stable heritable phenotypes with chromosomal involvement, but without directly changing the polynucleotides (Berger et al., 2009). The resulting epigenetic marks can also be passed on to daughter cells. The main strategies include altered gene expression by DNA methylation or histone modification (Yun et al., 2011). These changes may occur naturally, but are invariably influenced by age, lifestyle, diseases or environment. Lately, consecutive data revealed that epigenetically modified chromatin states are linked with disparate illnesses. Some of them are filed by the term “genomic imprinting”: In mammals, there are genes for which the maternal and paternal gene copy differs from each other and when mutations occur, they can clinically result in the shape of syndromes as “Angelman’s“ or “Prader-Willi”(Bonello et al., 2017). Additionally, epigenetic regulatory elements play a role in DNA repair genes or in the control of cell cycle and thereby support cellular transition to harmful outgrowth and malignant progression. The structure of DNA methylation in cancer cells totally differs from normal cells: Essentially, methylation as the most prevalent modification occurs at CpG islands. In ill-natured cells, promoter hypermethylation proceeds in silencing of tumor suppressor genes and thus facilitates human cancer progression (Esteller, 2007). Hypomethylation also impairs the cell’s fate into a neoplastic direction. The second important epigenetic mechanism includes alteration of the DNA packaging. Normally, the deoxyribonucleic acids are wound around a double set of four histone proteins (H1, H2, H3 and H4) which together form one nucleosome. Specific marks, especially acetyl- or methyl-supplements, are added to the nucleosomes by definite enzymes and actuate the procedure of DNA replication (Fraga et al., 2005). Vice versa, also a decrease of functional groups on H3 and H4 enables tumorigenesis: Less entry on the assets sites of Lysine 4 (H3K4me3), Lysine 9 (H3K9me) and Lysine 27 (H3K27me3) by acetylation or (tri-)methylation

results again in the reticence of genes containing anti-tumorous potential. All in all, these modalities represent a common peculiarity of human neoplasia. For EwS, the specific translocation fusion proteins containing EWS/ERG motifs in the ESFT are known to be associated with the regulation of transcription by functioning as aberrant transcription factors. Riggi et al. reconciled the named key histone changes with the EWS-FLI1 binding sites and found them in large parts enriched for H3K27ac and H3K4me3; both are commonly used as markers for enhancer and transcriptional activity (Riggi et al., 2014). Therefore EWS-FLI1 directly influences the cells' global gene expression programs and boosts malignant behaviour and cancer formation. The underlying nucleobases were unmasked as repetitive GGAA motifs (microsatellites). Depending on the quantity of repeats, they serve as connective elements for EWS-FLI1 to activate or repress thousands of target genes mediating oncogenesis (Gangwal et al., 2008). This deregulation of the expression profile due to the power of mainly the EWS-FLI1 translocation product is an unique epigenetic feature of EwS and provides the opportunity for targeted epigenetic therapeutic approaches. Consequently, research in direct epigenetic anticancer treatment proceeded over the last decades. For example, the application of histone deacetylase inhibitors (HDAC inhibitors) revealed remarkable antitumorous effects (Sakimura et al., 2005; Schlottmann et al., 2012). Moreover the use of cyclin dependent kinase inhibitors (CDK inhibitors) led to a decreased growth and oncogenic dynamic of EwS (Kennedy et al., 2015). As a result, the epigenome is restructured, and a new pattern of histone modifications develops. This bar code is scanned by epigenetic readers, different types of proteins with the ability to pass the emerged epigenetic information. Anyhow, these reader proteins can act as recruiters or stabilizers in various nuclear processes such as mediating DNA strand coding or recombination and gene transcription repression through interaction with the nucleosomes (Musselman et al., 2012). They mostly contain bromodomains; components which deliver and transduce the modified histone codes. One of the most important bromodomain group is the bromodomain and extra terminal bromodomain family (BET family).

1.2.2 BRD bromodomain proteins

The BET family consists of BRD2, BRD3, BRD4 and BRDT and its members identify epigenetic marks by binding N-acetylated lysine rests in histones (Ntranos & Casaccia, 2016; Taniguchi, 2016). Isolated cDNA of BRD2, BRD3 and BRD4 can be found in several tissues and especially BRD4 can be seen as limitlessly expressed, though BRDT belongs merely to the testis (Shang et al., 2004). Each of

these proteins inhere two bromodomains at the N-terminal (Bromo1 and Bromo2) which are considered to mediate the bonding with the opened chromatin and one extra terminal domain. Moreover, BRD4 and BRDT possess an extra C-terminal motif (Belkina & Denis, 2012; Shi & Vakoc). The underlying structural motif of the BRD proteins is composed of a preserved amino acid domain folding one alpha helix and two loops. Separately, these modules carry four single chains which create an inner hydrophobic pocket (see **Figure 1 A/B**). Provided with this oppositely charged recognition site, BRD proteins adhere the H3 and H4 histone acetylated lysine residues and enable the communication between transcription factors and loose chromatin. Thereby the regulatory transcription complex is mastered (Dhalluin et al., 1999; Garnier et al., 2014; Sanchez & Zhou, 2009; Zeng & Zhou, 2002).

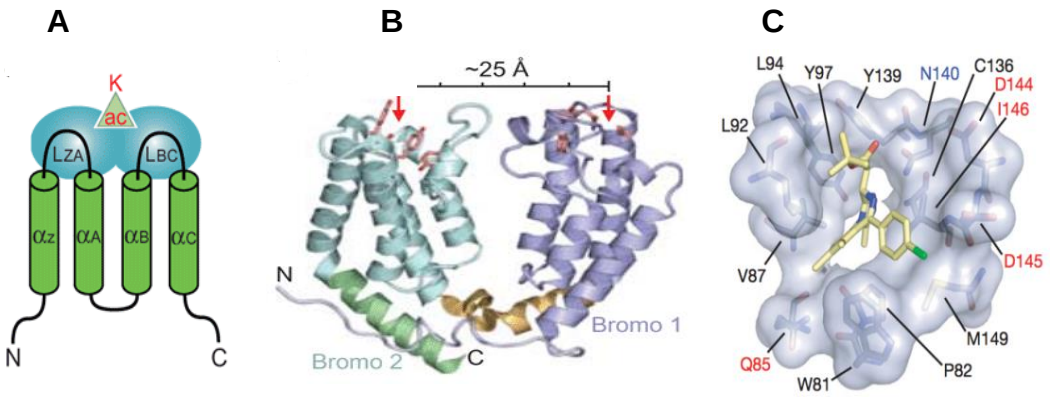

Figure 1: BET bromodomain proteins structure
A Schematic illustration of bromodomain typology: Alpha helices are colored in green (α_Z, α_A, α_B, α_C), the blue ovals represent the two loops (L_{ZA} and L_{BC}). All together they form the acetyl-lysine recognition and binding pocket which is approximately located at the green triangle (Taverna et al., 2007). **B** Tertiary structure of a typical reader protein: Two bromodomains ($Bromo_1$ and $Bromo_2$) generate a deep pocket at one side of the alpha helices bundle with a distance of approximately 25 amino acids (Taverna et al., 2007). **C** The image displays the acetyl-lysine binding pocket of BRD4. JQ1 as a potent inhibitor of BRD proteins blocking the catalytic reading center is colored in yellow (Filippakopoulos et al., 2010).

1.2.3 BRD proteins and their biological function

BET family members resemble each other regarding their primary sequence, tertiary folding structure and biochemical or cellular activities. Their similar key feature is binding modulated, hyperacetylated histones and activating chromatin for

transcription. On the other hand their properties result in different biological functions (Shao et al., 2016). To the current knowledge BRD2, previously known as Ring3/fsrg1, directly interacts with the transcription factor E2F and RNA polymerase II. Its subregions identify a lysine rest at the histone H4 acetylated on K5 and K12 and master the requirement of cyclin D1 (Nakamura et al., 2007). Strikingly, it does not loosen the connection (as BRD3 or BRD4) to the actively described chromatin, but stays strongly linked during mitosis (LeRoy et al., 2008)**.** Furthermore, it was shown that homozygous BRD2 and BRD4 deficient mouse models are embryonic lethal (Shang et al., 2011; Shang et al., 2009). Additionally it is discussed, whether BRD2 has other non-chromatin dependent functions as a cooperating partner in NF-κB pathways by tethering the protein RelA (v-rel avian reticuloendotheliosis viral oncogene homolog A) and by driving pro-inflammatory cytokines (Belkina et al., 2013). BRD3, as well as BRD2, binds to an overlapping subset of acetylated chromatin motives at H4 and H3 but BRD2 is related to another transcription factor named GATA1 to promote its chromatin occupancy (Lamonica et al., 2011; LeRoy et al., 2008). In addition, it was shown that one of the BRD3-bromodomains (BRD3R) uniquely directs reprogramming activity (Shao et al., 2016). The 200-kDa isoform protein encoded by BRD4 is homologous to the murine protein MCAP, which is conformed to associate with chromosomes during mitosis and disposes a serine/threonine kinase. A very prominent interaction of BRD4 with the P-TEFb (positive transcription elongation factor b) complex mediates active transcription via CyclinT1 and CDK9 (Jang et al., 2005; Lu et al., 2015). Furthermore BRD4 may support BRD2 in activating NF-kappaB (Huang et al., 2009) and is discussed to play a role in cell cycle regulation by association with RFC (replication factor C) (Maruyama et al., 2002). Lately investigations have confirmed BRD4 being preferentially situated at super enhancer regions which can either result in launching oncogenes or repressing tumor suppressors (Chapuy et al., 2013; Loven et al., 2013). These bipolar functions have recently also been found in EwS: EWS-FLI1 binds to common GGAA repeats in EwS and enables chromatin opening and facilitates boost-transcription through creating new super-enhancers. In contrast to “normal” enhancers, these super-enhancers inhere more power regarding TF arrangement, quantity and gene expression performance (Whyte et al.,

2013). In contrast EWS-FLI1 also removes wild-type ETS transcription factors from chromatin and suppresses differentiation (Riggi et al., 2014).

1.2.4 BET proteins are druggable targets

Recently, also the impact of epigenetic readers on the EWS-FLI1 binding sites has been investigated (Filippakopoulos et al., 2010; Greschik et al., 2017). Over the last decades, the function of epigenetic readers has become a place of interest for several pharmaceutically active small molecule inhibitors such as JQ1 and I-BET151. These newly developed agents have a similar chemical structure and a high affinity as being pan-BET family inhibitors: JQ1 and I-BET151 “mimic” acetylated histones. Thereby the bromodomains Bromo1 and Bromo2 are already blocked and the attraction of transcription factors to the activated chromatin is disabled (Filippakopoulos et al., 2010; Nicodeme et al., 2010), see **Figure 1C**. Primarily epigenetic readers have successfully been addressed with targeted pharmaceutical vehicles. This reversible obstruction of the catalytic acetyl-lysine binding domain displaces the chromatin complexes and conducts a protein-protein malinteraction. As a result the transcription initiation is arrested (Junwei & Vakoc, 2014; Muller et al., 2011; Padmanabhan et al., 2016). During the last years, they have shown promising antitumor potential and are expected to become promising candidates for epigenetic therapy. Additionally, collected data from BET inhibitors in clinical trials enhanced their prestige and inaugurated new strategies concerning ‘epigenetic therapy’. Several neoplastic entities, hematological diseases, solid tumors and cardiovascular inflammation are effectively addressed (Aristeidis Chaidos et al., 2015; Ferri et al., 2016). In vitro not only a remarkable decrease in tumor growth was noticed but also a down regulation of c-MYC expression and an increased rate of apoptosis (Delmore et al., 2011; Perez-Salvia et al., 2017; Zhu et al., 2017). C-MYC, as one of the strongest oncogenes and transcription factor, is known to influence cell cycle regulation, cell differentiation and survival (Gustafson & Weiss, 2010). In various cancer types, c-MYC is found to be overexpressed and therefore represents an attractive target. Normally, oncogenes are highly controlled by histone acetylation and superenhancers. Additionally, for c-MYC a communication between the BRD proteins has already been stated in some cancer types and an accurate targeting by BET inhibition (BETi) seems potential. Likewise

BRD4 was questioned to be associated in the regulation of c-MYC pathways and the induction of differentiation in different osseous cell lines (Zuber et al., 2011). In **Figure 2** the course is schematically displayed: BRD4 is dislocated by a suitable fragment and active transcription of the oncogene hindered (Ramadoss & Mahadevan, 2018). For EwS, c-MYC can also be found overexpressed. Consequently, BRD4 and the other members of the BET family portray favorable targets for treatment. In contrary, recent publications with the use of JQ1 did not show a diminished expression in EwS. Interestingly, on the contrary the oncogenic key driver fusion protein EWS-FLI1 was significantly down-regulated. The cell expansion in vitro and in vivo was declined, too (Hensel et al., 2016; Loganathan et al., 2016). As a conclusion, it can be said that there is an urgent need of unveiling the single BET family members' power and influence in EwS.

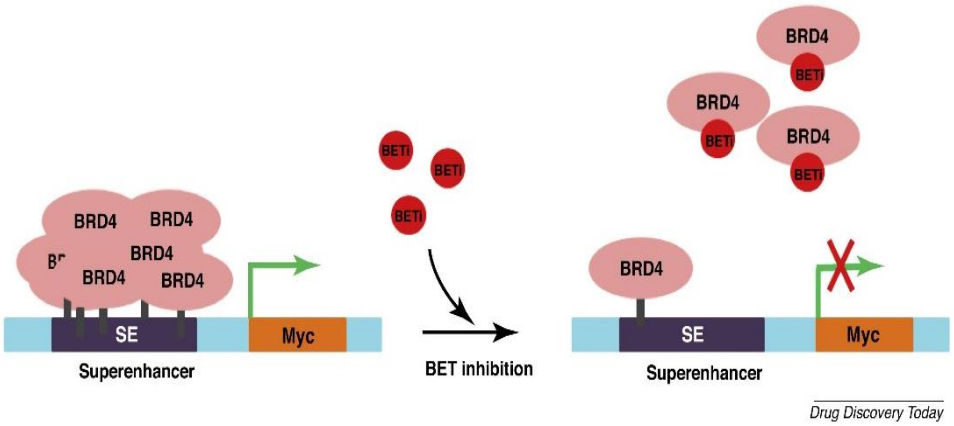

Figure 2: Super-enhancers are displaced by BET inhibition (Ramadoss and Mahadevan 2018)

1.3 Purpose of this study and working program

As the leading oncogenic fusion product EWS-FLI1 has proven of a substantial relevance on EwS tumor formation, it is seen as the master regulator of key mechanism in ESFT cancers (Burdach et al., 2009). Specifically, histones have been shown to undergo an alteration which is regulated by EWS-FLI1. Epigenetic readers, which act downstream of these bindings to specific modifications, are influenced as well. Interestingly, recent research demonstrated that pan-BET inhibitors can hijack the EWS-FLI1 expression and thereby downregulate the EwS mediated pathognomonic expression program (Hensel et al., 2016; Jacques et al., 2016; Loganathan et al., 2016). The aim of this work was to shed further light onto the relevance of each of the decoding proteins for tumorigenesis in EwS. Therefore, transient (siRNA) and constitutive (shRNA) knock-downs of BRD2, BRD3 and BRD4 in EwS cell lines were established to analyze to which extent single BRDs contribute to oncogenic transformation and malignancy and to acquire more knowledge on how BRD proteins are involved in maintaining the specific epigenetic landscape. Additionally, different BET inhibitors were on trial to evaluate possible analogies and to elucidate the potential underlying interdependencies with EWS-FLI1.

2 MATERIAL

2.1 List of manufacturers

Company	Locus
Abbott	Wiesbaden, Germany
Abcam	Cambridge, UK
Abnova	Taipei, Taiwan
ACEA	San Diego, California, USA
AEG	Nürnberg, Germany
Affimetrix	High Wycombe, UK
Ambion	Austin, Texas, USA
Amersham Biosciences	Piscataway, New Jersey, USA
Applied Biosystems	Darmstadt, Germany
ATCC	Rockyville, Maryland, USA
Autoimmun Diagnostika	Strassberg, Germany
B. Braun Biotech Int.	Melsungen, Germany
BD Bioscience Europe	Heidelberg, Germany
Beckman Coulter	Palo Alto, California, USA
Beckton Dickinson	Heidelberg, Germany
Berthold detection systems	Pforzheim, Germany
Biochrom	Berlin, Germany
Biometra	Göttingen, Germany
BioRad	Richmond, California, USA

Biozym	Hessisch Oldendorf, Germany
Brand	Wertheim, Germany
Calbiochem	Darmstadt, Germany
Carestream Health	Stuttgart, Germany
Cayman Chemical Company	Ann Arbor, Michigan, USA
Cell Signaling Technology	Frankfurt a. M., Germany
Clontech-Takara Bio Europe	Saint-Germain-en-Laye, France
Dako	Hamburg, Germany
DCS	Hamburg, Germany
DSMZ	Braunschweig, Germany
Elma	Singen, Germany
Eppendorf	Hamburg, Germany
Eurofins MWG GmbH	Ebersberg, Germany
Falcon	Oxnard, California, USA
Feather	Osaka, Japan
Fermentas	St. Leon-Rot, Germany
GE Healthcare	Little Chalfont, UK
GE Healthcare	Uppsala, Sweden
GeneArt	Regensburg, Germany
Genomed	St- Louis, Missouri, USA
Genscript	New Jersey, USA
Genzyme	Neu-Isenburg, Germany
GFL GmbH	Segnitz, Germany
Gibco	Darmstadt, Germany

GLW	Würzburg, Germany
Greiner Bio-One GmbH	Frickenhausen, Germany
Hamilton	Bonaduz, Switzerland
Heidolph Instruments	Schwabach, Germany
Heraeus	Hanau, Germany
ImmunoTools	Friesoythe, Germany
Implen GmbH	München, Germany
Invitrogen	Karlsruhe, Germany
Kern	Balingen-Frommern, Germany
Laborservice	Harthausen, Germany
Leica	Wetzlar, Germany
LGC Standards GmbH	Wesel, Germany
Life Technologies	Carlsbad, California, USA
LMS	Brigachtal, Germany
Lonza	Basel, Switzerland
Mabtech	Hamburg, Germany
Macherey-Nagel	Düren, Germany
Memmert	Schwabach, Germany
Merck	Darmstadt, Germany
Merck Millipore	Darmstadt, Germany
Metabion	Planegg-Martinsried, Germany
Miltenyi	Bergisch Gladbach, Germany
Mirus	Madison, Wisconsin, USA
Nalgene Rochester	New York, New York, USA

Nikon	Düsseldorf, Germany
Origene	Rockville, Maryland, USA
PAA	Cölbe, Germany
Peqlab	Erlangen, Germany
Perkin Elmer	Akron, Ohio, USA
Peske OHG	München, Germany
Philips	Hamburg, Germany
Promega	Madison, Wisconsin, USA
Qiagen	Chatsworth, California, USA
R&D Systems	Minneapolis, Minnesota, USA
Ratiopharm	Ulm, Germany
Roche	Mannheim, Germany
Roche	Penzberg, Germany
Roth	Karlsruhe, Germany
Santa Cruz Biotechnology	Heidelberg, Germany
Sarstedt	Nümbrecht, Germany
Sartorius	Göttingen, Germany
Scientific Industries	Bohemia, New York, USA
Scotsman	Milan, Italy
Sempermed	Wien, Austria
Sequiserve	Vaterstetten, Germany
Siemens	München, Germany
Sigma Aldrich	St. Louis, Missouri, USA
Stratagene	Cedar Creek, Texas, USA

Syngene	Cambridge, UK
Systec	Wettenberg, Germany
TaKaRa Bio Europe	Paris, France
Taylor-Wharton	Husum, Germany
Techlab	Braunschweig, Germany
Thermo Scientific	Braunschweig, Germany
Thermo Fisher Scientific	Braunschweig, Germany
TKA GmbH	Niederelbert, Germany
TPP	Trasadingen, Switzerland
VWR	Darmstadt, Germany
Whatman	Dassel, Germany
Zeiss	Jena, Germany

Table 1: List of manufacturers

2.2 List of general material

Material	**Manufacturer**
24 well non-tissue culture plate	Falcon
6 well tissue culture plate	Falcon
96 well cell culture plate	Greiner Bio-One
Cell culture flasks (25 cm^2, 75 cm^2, 175 cm^2)	Greiner Bio-One
Cell culture flasks (25 cm^2, 75 cm^2, 175 cm^2)	TPP
Cell culture flasks (75 cm^2, 175 cm^2)	Falcon
Cell strainer 40 µm	Falcon
Columns (MACS, LS and MS)	Miltenyi

Combs (Western blot)	Peqlab
Cryovials 1.5 ml	Sarstedt
Cryovials	Nunc
Culture dishes (NunclonTM surface 100 mm)	Nunc
Cuvettes	Roth
E-plate (96-well)	ACEA
E-plates (96-well)	Roche
Filters for solutions (0,2 µm, 0,45 µm)	Sartorius
Gloves (nitrile, latex)	Sempermed
Hybond-P PVDF membrane	GE Healthcare
Hypodermic needle (23 G, 30 G)	B. Braun
MultiScreen-HA Filter Plates	Merck Millipore
Parafilm	Pechiney Plastic Packaging
Pasteur pipettes	Peske OHG
Petri dishes	Falcon
Pipette filter tips (1000 µl, 200 µl, 100 µl, 20 µl,	Thermo Scientific
Pipette tips (1000 µl, 200 µl, 100 µl, 20 µl, 10 µl)	Molecular BioProducts
Pipettes (25 ml, 10 ml and 5 ml)	VWR
Plates for invasion-assay (24-well)	Becton Dickinson
Plates for qRT-PCR (96 well)	Applied Biosystems
Reagent reservoir (for 12 channel pipette)	VWR
Reagent reservoirs (50 ml)	Falcon
Syringes (27 G x 318 mm, 0,45 mm x 10 mm)	BD Biosciences
Syringes (29 G 0,33 mm x 12,7 mm)	B. Braun

Syringes (5 ml)	B. Braun
Syringes (GC, 1710LT)	Laborservice
Syringes (Hamilton 100 µl, 250 µl)	Techlab
Syringes (Omnifix-F, 9161406V)	B. Braun
Tubes for flow cytometry (5 ml)	Sarstedt
Tubes for PCR	Sarstedt
Whatman paper	Whatman

Table 2: List of general material

2.3 List of used instruments and equipment

Device	Designation	Manufacturer
Airflow	-	Köttermann
Autoclave	V95	Systec
Autoclave	2540EL	Systec
Bacterial shaker	Certomat BS-T	Sartorius
Cell counting chamber	Neubauer	Brand
Centrifuge	Multifuge 3 S-R	Heraeus
Centrifuge	Biofuge fresco	Heraeus
Controlled freezing box	Mr. Frosty	Nalgene
Drying cabinet	-	Memmert
Electrocorporater	Nucleofactor I	Amaxa biosystems
Electrocorporator	Gene Pulser XCellTM	BicRad
Electrophoresis chamber	-	BioRad
Flow cytometer	FACScalibur	Becton Dickinson

Fluorescence Microscope	AxioVert 100	Zeiss
Freezer –20°C	Cool vario	Siemens
Freezer -80°C	Hera freeze	Heraeus
Fridge +4°C	Cool vario	Siemens
Gel documentation	Gene Genius	Syngene
Heating block	Thermomixer Comfort	Eppendorf
Hemocytometer	Neubauer	Brand
Ice machine	AF 100	Scotsman
Incubator	Hera cell 150	Heraeus
Incubator	B20	Heraeus
Liquid nitrogen reservoir	L-240 K series	Taylor-Wharton
Luminometer	Sirius Luminometer	Berthold detection systems
Microliter syringe	710NR	Hamilton
Micropipette 0,5 - 10 µl	-	Eppendorf
Micropipette 10 - 100 µl	-	Eppendorf
Micropipette 100 - 1000 µl	-	Eppendorf
Micropipette 20 - 200 µl	-	Eppendorf
Microscope	DMIL	Leica
Microscope	AxioVert 100	Zeiss
Microwave/Oven	-	Siemens AEG
Mini Centrifuge	MCF-2360	LMB
Multichannel pipette 10 - 100 µl	-	Eppendorf
PCR cycler	-	Eppendorf
PCR cycler	Cycler	BicRad

Pipetting assistant	Stripettor Plus	Falcon
Pipetting assistant	Easypet	Eppendorf
Power supplier	Standard Power Pack	Biometra
qRT-PCR cycler	7300 Real-Time PCR	Applied Biosystems
Rotator	-	GLW
Scales	770	Kern
Scales	EW3000-2M	Kern
SDS-PAGE Chamber	Minigel-Twin	Biometra
Semi-Dry Transfer Apparatus	Fastblot	Biometra
Shaker	Polymax 2014	Heidolph Instruments
Sonifier	S60H Elmasonic	Elma
Spectrophotometer	GeneQuant II	Amersham Bioscience
Sterile bench	-	Heraeus
Vortexer	Vortex-Genie 2	Scientific Industries
Water bath	-	GFL
Water purification system	TKA GenPure	TKA GmBH
Western blot documentation	GelLogic1500 imaging	Carestream Health, Inc.
Western blot Detection system	-	GE Healthcare
xCELLigence system	-	Roche/ACEA Biosciences

Table 3: List of used instruments and equipment

2.4 List of chemical and biological reagents

Agent	**Manufacturer**
1-bromo-3-chloropropan (BCP)	Sigma

37% Formaldehyde	Merck
Acrylamide 30%	Sigma
Agar	Sigma
Agarose	Invitrogen
AIM-V Medium	Invitrogen
Ammonium persulfate (APS)	Sigma
Ampicillin	Merck
ampliTaq DNA Polymerase	Invitrogen
autoMACSTM Rinsing Solution	Miltenyi
BenchMarkTM Prestained Protein Ladder	Invitrogen
Blue Juice Gel Loading Buffer	Invitrogen
Bradford reagent	BioRad
Bromophenol Blue	Sigma
Butylated hydroxyanisole (BHA)	Sigma
Calcein AM	Merck
Diethyl Pyrocarbonate (DEPC)	Sigma
Dimethyl Formamide	Roth
Dimethyl Sulfoxide (DMSO)	Merck
D-Luciferin	Perkin Elmer
DMEM medium	Invitrogen
dNTPs	Roche
Doxycycline	Merck
Ethanol	Merck
Ethidium bromid (EtBr)	BioRad

Ethylen-Diamine-Tetra-Acetate (EDTA)	Invitrogen
Fetal Bovine Serum (FBS)/Fetal Calf Serum (FCS)	Biochrom
Ficoll-Paque	GE Healthcare
Gentamycin	Biochrom
Glycerol	Merck
Glycine	Merck
Hank's Buffered Salt Solution (HBSS)	Invitrogen
HEPes	Sigma
Hexadimethrine Bromid (Polybrene)	Sigma
HiPerFect Transfection Reagent	Qiagen
Human IgG	Genzyme
Human male AB serum	Lonza
Hydrochlorid Acid (HCL)	Merck
Isofluran	Abott
Isopropanol	Sigma
L-Glutamin	Invitrogen
MACS® BSA Stock Solution	Miltenyi
Magnesiumchlorid ($MgCl_2$)	Invitrogen
Matrigel Matrix	BD Biosciences
MaximaTM Probe/ROX qRT-PCR Mastermix (MM;	Fermentas
Methanol	Roth
Methylcellulose	R&D Systems
Natrium-Pyruvate	Invitrogen
N-N-N'-N'-Tetramethylethan-1,2-diamin (TEMED)	Sigma

Non-esssential Amino Acids (NEAA)	Invitrogen
Paraformaldehyde (PFA)	Merck
PCR buffer 10x	Invitrogen
Penicillin/Streptomycin	Invitrogen
Peptone	Invitrogen
Phosphate buffered saline (10 x PBS)	Invitrogen
Polyacrylamide (30% Acrylamide/Bis)	Merck
Propidium Iodide (PI)	Sigma
Prostaglandin E2 (PGE_2)	Cayman Chemical Company
Protease Inhibitor	Roche
Proteinase K	Sigma
Puromycin	PAA
Ready-Load 1KB plus DNA Ladder	Invitrogen
Ribonuclease A (RNaseA)	Roche
RNA Gel Loading Dye (2x)	Thermo Fisher Scientific
RPMI 1649 medium	Invitrogen
Skim milk powder	Merck
Sodium azide (NaN_3)	Merck
Sodium chloride	Merck
Sodium Dodecyl Sulfate Polyacrylamide (SDS)	Sigma
Sodium hydroxide (NaOH)	Merck
Tris	Merck
Triton X-100	Sigma
Trypan Blue	Sigma

Trypsin	Invitrogen
Tween 20	Sigma
TWS 119	Merck
β_2-microglobulin	Sigma
B-Mercaptoethanol	Sigma

Table 4: List of chemical and biological reagents

2.5 List of commercial reagents

Kit	**Manufacturer**
AccuPrime Taq DNA Polymerase System	Invitrogen
Affymetrix GeneChip Whole Transcript Sense Target	Affimetrix
Annexin V-PE Apoptosis Detection Kit I	BD Biosciences
BioCoat™ Angiogenesis System	BD Biosciences
Cell Invasion Assay	BD Biosciences
Cell proliferation ELISA BrdU Kit	Roche
ECL-Plus Western Blot Detection System	GE Healthcare
EndoFree ® Plasmid Maxi Kit	Qiagen
GeneChip Whole Transcript Sense Target Labeling Kit	Affymetrix
High-Capacity cDNA Reverse Transcription Kit	Applied Biosystems Thermo Fisher Scientific AG
Human Methylcellulose Base Media	RD Systems
JETSTAR 2.0 Plasmid Maxiprep Kit	Genomed
Labeling Kit	Affimetrix
MycoAlertTM Mycoplasma Detection Kit	Lonza
One Shot® TOP 10 E. coli strain (chemically competent)	Invitrogen

RNeasy® Mini Kit	Qiagen
TaqMan® Gene Expression Assays	Applied Biosystems
TRI Reagent RNA Isolation Kit	Ambion

Table 5: List of commercial reagents

2.6 Media, buffers and solutions

2.6.1 List of universal solutions

Name	Ingredients
1 x Trypsin	45 ml of PBS, plus 5 ml 1 / 10 trypsin
1 x PBS	900 ml autoclaved water, plus 100 ml 10 x DPBS

Table 6: List of universal solutions

2.6.2 List of cell culture media

Name	Ingredients
Standard tumor medium	500 ml of either a) RPMI 1640 medium or b) DMEM medium, plus 10% FCS, plus 100 U/ml penicillin and 100 µg/ml streptomycin
Standard freezing medium	FCS plus 10% DMSO
LB-Medium	1l of distillated H2O, plus 10 g NaCl, plus 10 g Pepton, plus 5 g Yeast-extract; auto-claved; stored at RT

Table 7: List of cell culture media

2.6.3 List of Western blot reagents

Name	Ingredients
2 x Laemmli	2 ml Glycerol, plus 0,5 M Tris-HCl (pH 6,8), plus 4 ml 10% (w/v) SDS, plus 0,5 ml 0,1% (w/v) BPB, plus 5% β-mer-capto-ethanol, plus H_2O; stored at RT
10% SDS	90 ml of autoclaved H_2O, plus 10 g SDS
5 x transfer buffer	36,05 g Glycine, plus 7,5 g Tris, pH: 8,3; stored at RT
5 x running buffer	15,14 g Tris, plus 57,05 g Glycine, plus 5 g SDS; pH: 8,5; stored at RT
4 x separating buffer	9,08 g Tris, plus 0,2 g SDS, pH: 8,8; stored at RT
4 x stacking buffer	3,03 g Tris, plus 0,2 G SDS, pH: 6,8; stored at RT
10 x TBS	1000 ml of distillated H_2O, plus 87,6 g NaCl, plus 12,1 g Tris; pH: 8,0; stored at RT
1 x TBS	900 ml of distillated H_2O, plus 100 ml of 10 x TBS; stored at RT
1 x TBS-T	900 ml of distillated H_2O, plus 100 ml of 10 x TBS, plus 500 µl Tween 20; stored at RT
5% skimmed milk with 0,05% Tween 20	300 ml of 1 x TBS-T, plus 15 g skimmed milk powder; stored at 4°C
Separating gel (10%)	6,2 ml of 30% Acrylamide, plus 4 ml of 4 x separating buffer, plus 5,6 ml of H_2O, plus 50 µl APS (10%) and 20 µl TEMED; stored at RT

Stacking gel	1,5 ml of 30% Acrylamide, plus 2,5 ml of 4 x stacking buffer, plus 6 ml H_2O, plus 50 µl APS (10%) and 20 µl TEMED; stored at RT
APS 10%	1000 µl H_2O, plus 0,1 g Ammoniumpersulfat; stored at 4°C

Table 8: List of Western blot reagents

2.6.4 List of flow cytometry solutions

Name	Ingredients
Sample buffer	1 l of 1 x PBS, plus 1 g Glucose; filtered through a 0,22 µm filter; stored at 4°C
20 x PI stock solution	100 ml H_2O, plus 100 mg propidium iodine, filtered through a 0,22 µm filter; stored at 4°C
RNAse A	1 ml H_2O, plus 32,5 mg RNAse A; aliquoted and stored at -20°C
1 x PI staining solution	1 ml cold sample buffer, plus 0,05 ml 20 x PI stock solution, plus 32 µl RNAse A
Standard staining buffer	PBS, plus 0,05% NaN_3, plus 2% FCS; stored at 4°C

Table 9: List of flow cytometry solutions

2.6.5 List of electrophoresis reagents

Name	Ingredients
50 x TAE Buffer	2 M Tris, 10% EDTA (0,5 M), 5,71% HCl
1 x TAE	20 ml of 50 x TAE, plus 980 ml DEPC-H_2O
Electrophoresis gel	60 ml 1 x TAE, plus 0,7 - 1% Agarose , plus 2 µl EtBr

Table 10: List of electrophoresis reagents

2.7 List of Western blot antibodies

2.7.1 List of primary antibodies

All western blot antibodies were stored either at -4°C or at -20°C dependent on the manufacturer's advice.

Name	Type	Molecular weight	Dilution range	Company	Product number
BRD2	Monoclonal; rabbit	110 kDa	1:1000	Cell Signaling	5848
BRD2	Monoclonal; mouse	80 kDa	1:100/1:500	Santa Cruz	Sc-81202
BRD3	Polyclonal; rabbit	80 kDa	1:1000	Abcam	ab71815
BRD3	Polyclonal; Rabbit	80 kDa	1:1000	Bethyl	A302-368A-T
BRD4	Polyclonal; rabbit	152 KDa/80 kDa	1:100/1:1000	Santa Cruz	sc-48772
BRD4	Monoclonal; rabbit	200 kDa	1:1000	Cell Signaling	13440
BRD4	Monoclonal; rabbit	152 kDa	1:1000	Abcam	ab128874
β-Tubu-lin	Monoclonal; rabbit	55 kDa	1:1000	Cell Signaling	15115
HPRT	Polyclonal; rabbit	23 kDa	1:100/1:1000	Santa Cruz	sc-20975

FLI1	Monoclonal; rabbit	52 kDa	1:1000	Cell Signaling	35980
PARP	Monoclonal, rabbit	116 kDa	1:1000	Cell Signaling	9532
Casp-7	Monoclonal, mouse	20 kDa (cleaved30 kDa)	1:100	Cell Signaling	9494

Table 11: List of primary Western blot antibodies

2.7.2 List of secondary antibodies

Name	Dilution range	Company	Product number
goat anti-mouse	1:1000	Santa Cruz	sc-2060
Bovine anti-rabbit	1:1000	Santa Cruz	sc2370

Table 12: List of secondary Western blot antibodies

2.8 List of siRNA

All siRNAs were purchased from Qiagen and were stored at -20°C. Final concentrations were 5 nM, 10 nM and 13,5 nM respectively.

siRNA	Target Sequence
Negative non-silencing siRNA	5´-AATTCTCCGAACGTGTCACGT-3`
Hs_BRD2_8	5’-AAGTAGCAGTGTCACGCCTTA-3’
Hs_BRD3_8	5’-ACGCCGCCTGTCGTCAAGAAA-3’
Hs_BRD4_9	5’-ATGGACTAGAAACTTCCCAAA-3’

Table 13: List of siRNA

2.9 TaqMan Gene Expression Assays for qRT-PCR

All TaqMan primers for qRT-PCR were purchased from Applied Biosystems and were used with concentrations of 900 and 250 nM, respectively.

Primers	Gene Assay ID
DKK2	Hs00205294_m1
GAPDH	Hs99999905_m1
IFITM1	Hs01652522_g1
ISG15 (G1P2)	Hs00192713_m1
RANKL	Hs00243522_m1
TGFβ	Hs00998133_m1
HOX 10	Hs00157974_m1
BRD2	Hs01121986_g1
BRD3	Hs00201284_m1
BRD4	Hs04188087_m1
STEAP1	Hs00185180_m1
PAPPA	Hs00535718_m1
GPR64	Hs00971379_m1
c-MYC	Hs00153408_m1
EZH2	Hs01016789_m1

Table 14: List of TaqMan Gene Expression Assay primers

2.10 Bacterial strains

For plasmid multiplication, the chemically competent assay kit One Shot® TOP 10 E. coli strain (Invitrogen) was used to establish stable knock-down by retroviral gene transfer.

Corresponding genotype: F-mcrA Δ(mrr-hsdRMS-mcrBC) φ80lacZΔM15 ΔlacX74 recA1 araD139 Δ(araleu) 7697 galU galK rpsL (StrR) endA1 nupG.

2.11 HEK293T cells

This cell type is a variant of the HEK293 cell line. These cells are largely used for the generation of specific retroviral vectors. As a modification, HEK293T cells hold the SV40 Large T-antigen. This feature allows the replication and amplification of transfected plasmids. For cell treatment cells were seeded at 1x105 cells and treated with DMEM medium (Invitrogen) containing 10% FCS. The viral supernatant was taken 48 h after transfection and was used for assays involving retroviral gene transfer. The leftover was stored at -80°C.

2.12 pTRIPZ inducible lentiviral shRNA vector information

The design combines a microRNA-adapted shRNA with a TRIPZ lentiviral doxycycline inducible vector to generate stable gene silencing. The vector was obtained from GE Healthcare (**Figure 3**).

2.12.1Schematic illustration

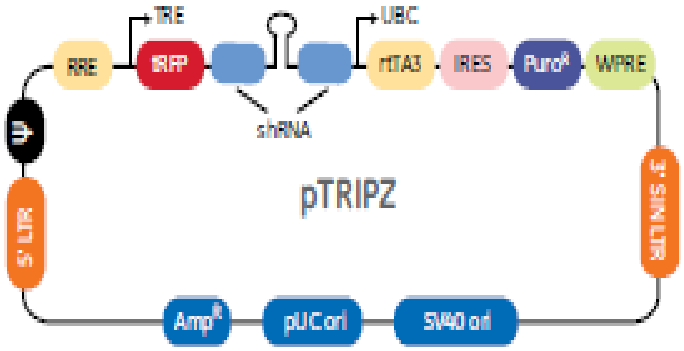

Vector Element	Utility
TRE	Tetracycline-inducible promoter
tRFP	TurboRFP reporter for visual tracking of transduction and shRNA expression
shRNA	microRNA-adapted shRNA (based on miR-30) for gene knockdown
UBC	Human ubiquitin C promoter for constitutive expression of rtTA3 and puromycin resistance genes
rtTA3	Reverse tetracycline-transactivator 3 for tetracycline-dependent induction of the TRE promoter
Puro^R	Puromycin resistance permits antibiotic-selective pressure and propagation of stable integrants
IRES	Internal ribosomal entry site allows expression of rtTA3 and puromycin resistance genes in a single transcript
5' LTR	5' long terminal repeat
3' SIN LTR	3' self-inactivating long terminal repeat for increased lentivirus safety
Ψ	Psi packaging sequence allows viral genome packaging using lentiviral packaging systems
RRE	Rev response element enhances titer by increasing packaging efficiency of full-length viral genomes
WPRE	Woodchuck hepatitis posttranscriptional regulatory element enhances transgene expression in the target cells

Figure 3: TRIPZ shRNA vector information
Source: GE Healthcare Inducible Dharmacon ™ TRIPZ ™ Lentiviral shRNA manual

2.12.2 Detailed vector map

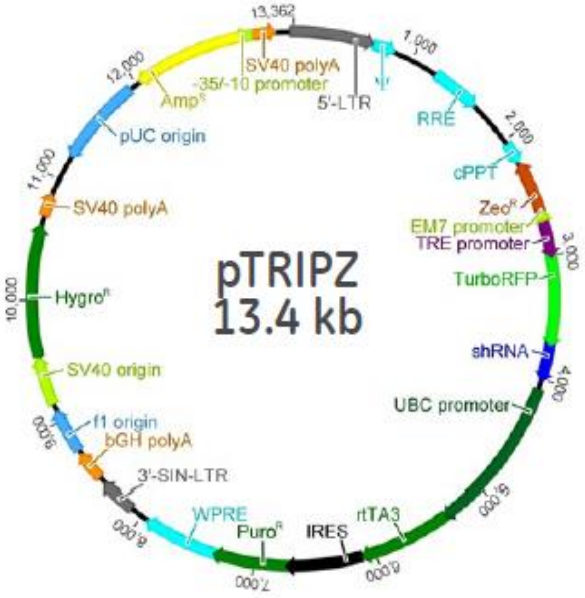

Figure 4: TRIPZ shRNA vector information
Source: GE Healthcare Inducible Dharmacon ™ TRIPZ ™ Lentiviral shRNA manual

2.13 List of human cell lines

All human cell lines were gained from the DSMZ (German Collection of Microorganisms and Cell Cultures). A673 was obtained from ATCC (LGC Standards).

Cell line	Description
A673	EwS adherent cell line characterized by type 1 translocation and gained from the primary tumor of a 15-year-old female patient and possesses a p53 mutation.
SK-N-MC	EwS adherent cell line with type 1 translocation derived from the neuroepithelial Askin's tumor metastasis (supraorbital) of a 14-year-old Caucasian girl; the Askin's tumors belong to the ESFT.
TC-71	Cell line established from the tumor of a 22-year-old man with metastatic Ewing sarcoma (humerus).

Table 15: List of human cell lines

3 METHODS

3.1 Human cell lines

EwS cell lines named TC-71 and SK-N-MC were received from the DSMZ (Deutsche Sammlung von Mikroorganismen und Zellkulturen GmbH), the German Collection of Microorganisms and Cell Cultures. A673 was gained from ATCC (LGC Standards). The retroviral packaging cell line HEK293T was purchased from Invitrogen.

3.2 Cell culture

The EwS cell lines A673, SK-N-MC and TC-71 were cultured in RPMI 1640 medium (Invitrogen) containing 10% FCS (Biochrom) and 1% P/S (100 U/ml penicillin and 100 µg/ml streptomycin; Invitrogen). The retroviral packaging HEK 293T cells were plated in DMEM (Invitrogen) containing 10% FCS, 1mM Na-Pyruvate,1mM non-essential amino acids and antibiotics. All cell lines were seeded in middle or large plastic flasks (Greiner Bio One) containing either 10 ml or 20 ml medium. They were grown under a humidified atmosphere (37°C and 5% CO_2). Cells were split every 3-4 days and re-seeded in fresh medium and new flasks in a dilution range from 1:2 up to 1:10 according to the following protocol: First the medium was discarded, and the cells were washed with 5 ml PBS to remove cell trash and used medium, second 5 ml 1 x trypsin were added and incubated at 37°C and 5% CO_2 for 5 min to dissolve adherent cells from the bottom. Furthermore, detached cells were gained with 10 ml standard RPMI tumor medium to harvest them in 50 ml tubes, followed by a centrifugation step at 1500 x g for 5 min to achieve pelleted cells. Finally, cells were re-suspended in fresh medium, counted for later analysis and then spread into new culture plastic flasks.

3.3 Freezing and thawing

Cells were resuspended in FCS containing 10% DMSO for later analysis. 500 µl of the solution were aliquoted in cryovials and were stored in an ethanol-controlled freezing box for 48 h at -80°C before transferring them into storage boxes for long

term conservation. Reculturing was performed firstly by thawing vials at RT, secondly by washing the incurred cell solution with 10 ml standard RPMI medium in the purpose to clean the cells from DMSO and finally by centrifuging samples at 1500 x g for 5 min. The cell pellet was resuspended in fresh medium and cultured in plastic cell flasks as described above in a humidified atmosphere (37°C/5% CO_2). Regularly cells were counted with a Neubauer hemocytometer and the use of trypan blue (Sigma) exclusion method. To ensure the purity of the tumor cells the cultures were frequently probed to check present EWS-FLI1 product. Additionally, the MycoAlertTM Mycoplasma Detection Kit (Lonza) was regularly used as described in the manufacturer's protocol to exclude mycoplasma contamination.

3.4 Transient transfection with siRNA

For transient RNA interference the HiPerFect Transfection Reagent was used according to the manufacturer's protocol. 2 x 10^6 cells were plated in a 10 mm cell culture dish at a total volume of 10 ml RPMI medium containing 10% FCS and 1% P/S and incubated 30 min at 37°C 5% CO_2. Afterwards adherent cells were treated with small interfering RNA (siRNA) in different concentrations (TC-71 13,9 nM; SK-N-MC and A673 5-10 nM). To enable cell penetration 36 µl (5 nM), 72 µl (10 nM) or 100 µl (13,9 nM) HiPerFect transfection solution was used. Interference efficiency was measured by RNA and/or protein extraction after an incubation for 12-72 h (mostly 48 h) at 37°C and 5% CO_2. Afterwards cDNA editing was performed as described below and quantitative Real-Time-PCR was used to detect gene silencing on RNA level or Western blot (WB) assay was performed for examining results on protein level. Samples were compared to control siRNA (negative siRNA, NEG). Several siRNAs with slightly different targets were tested (see **Table 13**: List of siRNA) to achieve highest transient knock-down.

3.5 RNA-Isolation using TRI Reagent RNA Isolation Kit

RNA isolation was performed by using the TRI Reagent RNA Isolation Kit according to the manufacturer's instructions (Ambion Manual Version 0610). First the medium was discarded and the cells were washed with PBS. Afterwards they were trypsinized and incubated at 37°C and 5% CO_2 for 5 minutes. Cell pellet was

resuspended in 1 ml TRI reagent and incubated at room temperature (RT) for 5 min. Per 1 ml TRI reagent 100 µl BCP (1-bromo-3-chloropropane) were added followed by a vortexing step and again by an incubation at RT for 5 up to 10 min. After the incubation samples were centrifuged at 12000 x g for at least 15 min at 4°C and the resulting aqueous phase was transferred into fresh tubes. To precipitate the RNA 500 µl isopropanol were used per 1ml of TRI reagent and then well mixed. Samples were incubated for 5 min at RT and centrifuged for 8 min at 12000 x g. Supernatant was discarded and the pellet was washed with 1 ml 75% ethanol by centrifuging at 7500 x g for 5 min. Finally, the ethanol was dismissed, and the RNA pellet was briefly air-dried before dissolving in 20-40 µl DEPT H_2O. Concentration and purity of RNA was measured photo-metrically at 260 nm and samples were stored at -80°C.

3.6 cDNA

To check genomic knock-down RNA must be transcribed into cDNA by using the High Capacity cDNA Reverse Transcription Kit (Thermo Fisher Scientific AG) as described in the manufacturer's handbook. Per 1 µg of RNA a master mix containing 2 µl 10 x RT buffer, 2 µl 10 x RT Random Primers, 1 µl dNTP-Mix (100 mM) and 0,8 µl MultiScribe™ Reverse Transcriptase (RT) was produced and mixed with RNAse free water to a total volume of 20 µl. cDNA synthesis was enabled by thermal cycling under the following conditions 10 min 25°C; 120 min 37°C; 5 min 85°C; ∞ 4°C. To examine gene expression cDNA was used for qRT-PCR and stored at -20°C for later additional analysis.

3.7 qRT-PCR

The qRT-PCR analysis was performed using Maxima™ Probe/ROX qPCR Master Mix (2x) (containing Hot Start Taq DNA Polymerase, PCR buffer and dNTPs) and specific TaqMan® Gene Expression Assays (Applied Biosystems) which consist of two unlabeled PCR primers and a FAM™ dye labeled TaqMan® MGB probe. 0,5 µl purified cDNA samples were analyzed in a 96-well plate and paired with 19,5 µl reaction mix containing 10 µl Maxima™ Probe/ROX qPCR Master Mix (2x), 1 µl TaqMan® Gene Expression Assays and 8,5 µl nuclease-free H_2O. For examining

gene expression of EWS-FLI1 the reaction mix varied as follows: 10 µl Maxima™ Probe/ROX qPCR Master Mix (2x), 7,9 µl nuclease-free H_2O. 0,6 µl forvert primer, 0,6 µl reverse primer and 0,4 µl sonde. The fluorescence was detected and measured in Step One Plus Real-Time PCR using a three-step cycling protocol: 1 s 50°C; 10 min 95°C; [15 s 95°C; 1 min 60°C] 40 x (Applied Biosystems). All samples were done as duplicates. The results were set in relation to the housekeeping gene glyceraldehyde 3-phosphate dehydrogenase (GAPDH) and assessment was performed by using the 2-ddCt method in Microsoft Excel; standard t-test showed the statistical significance.

3.8 Proliferation assay

Specific inhibition of cell growth by silencing different BET-bromodomain proteins (TRIPZ shRNA) or BET-inhibitors (I-BET151/dBET) was visualized by measuring the variance of impedance on golden microelectrodes based on the xCELLigence system (Roche/ACEA Biosciences, Basel, Switzerland). Cells were seeded in 200 µl medium containing 10% FCS. For A673 7,5 x 10^3 cells were plated, for SK-N-MC 1 x 10^4cells and for TC71 5 x 10^3 cells per well. TRIPZ Cells were treated three days in advance with doxycycline (at a final concentration of 1 µg/ml) for the purpose to ensure highest knock-down as described above or inhibitors were added and incubated at 37°C/ 5% CO_2 for seven days. xCELLigence instrument measured cell proliferation by specific cellular impedance every hour. Experiments were performed in sextuplicate.

3.9 Western blot

The protein sample preparation was done by the following process: The sample cells were washed once with 5 ml 1 x PBS and dealt with 5ml trypsin. The cells were harvested on the final concentration of 1 x 10^6 cells and were denatured by resuspension in 200 µl 2x Laemmli Buffer containing 10% SDS detergent. 50 µl 2-mercapto-ethanol were added per 1 ml Laemmli Buffer solution to reduce the intermolecular and intramolecular disulfide bonds. Samples were rocked gently at 70°C for 10 min and protein lysates were homogenized with a 23-gauge needle. Protein samples were either immediately transferred firstly to SDS-page and then

transmitted onto nitrocellulose membrane (Thermo Fisher AG) or stored at -80°C for later analysis. 10% polyacrylamide gels were hand casted and filled with 15-20 µl protein extracts and a prestained molecular weight standard marker (see **Table 11**: List of primary Western blot antibodies). By connecting to a gel electrophoresis system for 1,5-2 h (90 V/40 mA) the negatively charged samples were separated by molecular weight. Resulting bands were transferred electrically to a 30-sec ethanol-activated Hybond-PVDF membrane which is placed respectively between two Whatman filter papers (soaked in 1 x transfer buffer (see **Table 8**: List of Western blot reagents)) for 1,5 h at 200 mA. The membrane was incubated in 5% skimmed milk with 0,05% Tween 20 at RT for 1 h to block unspecific binding sites. For detecting protein banners two antibodies were used consecutively: First the membrane was paired with the fitting dilution (1:100 up to 1:1000) of the primary antibody (monoclonal rabbit/mouse anti-BRD IgG (see **Table 11**: List of primary Western blot antibodies)) in skimmed milk at 4°C for 4 h or overnight. Subsequently, the membrane was washed three times for 5 min in TBS-T before incubating with the correct secondary polyclonal rabbit/mouse antibody in 5% skimmed milk with 0,05% Tween 20 at RT for 1 h. Similarly the membrane was washed as described above two times in TBS-T, followed by one washing step (5-10 min) in TBS before visualizing the incidental bands using the ECL-Plus Western Blotting Detection System (GE Healthcare Booklet RPN2132PL Rev D 2006): Due to the antibody-antigen complexes the protein samples were visualized by luminescence (ECL chemiluminescence reagent) which is based on the oxidation of a Luminogen by HRP and peroxide; finally chemiluminescent signals were detected and analyzed by a CCD camera. β-Tubulin was used as loading control.

If the membrane was used twice to investigate more than one protein on the same blot it was immersed in 1 x Stripping Buffer for 12 min to remove primary and secondary antibody, washed twice (~ 5 min in TBS-T), blocked again in skim milk (~1 h) and reloaded with antibodies of interest as currently described.

3.10 I-BET151/dBET

For each cell line 2 x 10^6 cells were seeded in a 10 mm plate dish with RPMI medium to a total volume of 10 ml and incubated for 30 minutes. Afterwards the BET-

Inhibitor was added in different concentrations (1 nM, 2 nM and 5 nM). Cells were incubated 1-48 h at 37°C and 5% CO_2. All cell lines were treated in the same way with DMSO, which serves as a negative control. To measure inhibition efficiency either RNA was isolated, and RT-PCR was used to detect gene silencing on mRNA level or WB analysis was performed.

3.11 Colony forming assay

1 x 10^4 cells were suspended in 20 µl RPMI medium and added to 300 µl cell re-suspension solution containing the favored siRNA inhibitor. The mix was incubated for 8 min in a humidified atmosphere (37°C, 5% CO_2) and then transferred into 3 ml methylcellulose-based media, thoroughly vortexed and followed by an incubation step at 4°C for 60 min. Finally, the whole mixture was plated into two 35 mm plates with a total volume of 1,5 ml and cultured for 14 days at 37°C (5% CO_2). For examination of growth photos were taken and the number of colonies was analyzed with FiJi imaging processing package.

3.12 Cell cycle analysis

FACS analysis was used to check cell cycle process. Samples were cleared with PBS, trypsinized and centrifuged at 12000 x g for 5 min. The pellet was resolved and washed in cold sample buffer (see **Table 9:** List of flow cytometry solutions) several times (~2-3 x) before the cells were counted and cell concentration was adjusted at 1-3 x 10^6 cells/ml. 1 ml was taken and centrifuged at 4°C for 10 min. The supernatant was carefully discarded without touching the pellet. After vortexing vigorously for 10 sec the cells were fixed drop by drop in 70% ethanol over night at 4°C for maximal resolution. After the incubation the samples were spun down at 2000 x g for 5 min and the ethanol was removed thoroughly. Previously the sediments were vortexed and 1 ml staining solution (containing 0,05 ml PI and 32 µl RNAse A) was added. Before analyzing samples an incubation step for 30-60 min at RT was performed while gently rocking to ensure PI staining and RNA degradation. Samples were analyzed within 24 h on a FACScalibur flow cytometer (Becton Dickinson) with at least 20000 events/sample recorded. The Cellquest software (Becton Dickinson) enabled the evaluation.

3.13 Invasion assay

To examine the invasiveness of EwS the BioCoat™ Angiogenesis System “Endothelial Cell invasion kit” (BD Biosciences) was utilized. TRIPZ cells were stimulated with doxycycline (1 µg/ml) for in total 24 h. After thawing the 24-well assay plate at RT for 10 min the Matrigel membrane was rehydrated with 500 µl pre-warmed RPMI medium (without P/S and FBS) according to the manufacturer’s protocol. Then the cells were harvested and adjusted at 2 x 10^5/ml in supplementary free RPMI medium. The activated inserts were emptied carefully without touching the Matrigel membrane and then refilled with 250 µl cell suspension. Additionally, the lower chamber was loaded with 750 µl RPMI medium containing 10% FBS as a chemoattractant. Besides, some chambers without FBS were taken as negative controls. The assay kit was incubated at 37°C and 5% CO_2 for 48 h. The analyzation of the samples was performed using the fluorescence power of Calcein AM (final concentration 2 µg/ml): 25 ml of 37°C-preheated HBSS were mixed with 100 µl Calcein and the top of the assay plate was transferred into a new 24-well plate containing 1 ml staining solution per well, respectively. The kit was incubated without any light in a humidified atmosphere (37°C and 5% CO_2) for 90 min to permit the selective staining of the invasive cells on the bottom of the inserts. The results were visualized afterwards microscopically in 1 ml PBS by using a Zeiss AxioVert 100. Pictures were recorded with the attached AxioCam MRm and processed by the imaging program AxioVision (Zeiss). Every sample was done twice and 4 photos/well were reported before analyzing and counting the colonies with the image processing package FiJi.

3.14 Mini/Maxi plasmid preparation

For plasmid amplification lentiviral inoculums were picked from the E. Coli-glycerin-stock and transferred into 400 ml of LB-Medium containing 100 mg/ml ampicillin. Afterwards they were incubated at 37°C overnight while gently rocking. Further plasmid preparation was performed by using the EndoFree ® Plasmid Maxi Kit. Briefly, after >12 h of incubation the LB culture was harvested by centrifuging at 6000 x g and 4°C for 15 min; followed by a resuspension of the gained pellet. Additional steps were done as depicted in the manufacturer’s protocol. Finally, the

eluted and precipitated DNA was washed with 70% ethanol and then air-dried for 5-10 min. At the end they were redissolved in a suitable volume of endotoxin-free buffer and stored at -20°C. For checking the correct plasmid integration 3-5 µl of the plasmid DNA were run on a 1% agarose gel.

3.15 Establishing constant shRNA transfected TRIPZ cell lines

After having obtained the DNA by plasmid preparation as described above, a restriction enzyme digest was performed for diagnostic quality control of the TRIPZ Inducible Lentiviral shRNA vectors. Furthermore, a specific target sequencing followed to secure the content of the correct constructs. Finally, the cells were transfected according to the TRIPZ Inducible Lentiviral manual into HEK 293T retroviral packaging cell line and the resulting viral supernatant was taken 48 h after transfection. The gained viral liquids were used to generate stable knock-down of the targeting sequence before storing them at -80°C. Establishing constitutively shRNA expressing cell lines was done under the following conditions: 1×10^5 A673, SK-N-MC and TC-71 cells were plated in a 6-well plate in duplicates and were incubated at 37°C/5% CO_2 for 48 h. After achieving a final confluence of > 80 %, 1 ml of viral supernatant was added carefully and the transfected cells were grown in a humidified atmosphere for 48 h again. With the aim of separating and selecting successfully transfected antibiotic stable clones, the cells were treated with 2 µg/ml (standard RPMI tumor medium) puromycin for at least 14 days. Cell cultures were soon transferred into middle sized plastic culture flasks and were seeded in RPMI standard medium at 37°C and 5% CO_2 and grown under humidified conditions.

Best genomic silencing was gained by inducing the transfected cell lines 72 h in advance with 1 µg/ml doxycycline. The integration of the shRNA constructs and the resulting knock-down was observable by detecting the doxycycline-dependent Tet-on/Tet-off fluorescent signal with a fluorescent microscope. The positive presence of TurboRFP expression serves as a first indication of transfection efficiency. To check stable gene knock-down RNA was isolated, transcribed into cDNA compared to negative control shRNA (NEG) and qRT-PCR was performed as described above.

3.16 Agarose gel-electrophoresis

Agarose gel-electrophoresis was performed in the purpose of controlling the purity and quality of the isolated RNA: Commonly used gel conditions were 0,7% - 1% agarose dissolved in 60 ml of 1 x TAE buffer and boiled at 9000 watts for 2 min. After chilling at RT 2 µl EtBr were added, generously mixed and poured into the electrophoresis chamber to stack during 30 min. For every sample 1 µg of RNA was solved in 10 µl DEPC H_2O and brought together with 3 µl loading buffer (Thermo Fisher Scientific). The gel was run at 70 V for 20 min.

3.17 Microarray analysis

Microarray analysis was performed to detect changes in gene expression profiles due to genomic siRNA knock-down. SK-N-MC, A673 and TC-71 were treated with anti-BRD siRNA 48 h in advance, then RNA was isolated using the TRI Reagent RNA Isolation Kit and its purity checked by running on a 0,7% agarose gel. Additionally, total RNA was amplified and labeled using Affymetrix

GeneChip Whole Transcript Sense Target Labeling Kit was used as depicted in the provided manual. cRNA was paired to Affymetrix Human Gene 1.0 ST arrays and the gained data was subsequently analyzed using different microarray parsing tools (“Affimetrix software Suite 5.0”; genesis software packing). The “Significance Analysis of Microarrays” (SAM) showed modified gene expression. Additionally, GSEA (Gene set enrichment analysis) was run (http://software.broadinstitute.org/gsa).

3.18 Statistics

Prism 5 GraphPad Software was used to check data of mean, standard deviation and standard error of the mean, statistical analysis was performed with unpaired two-tailed student’s t-test. Settled statistically significant p-values: *$p < 0.05$; **$p < 0.005$; ***$p < 0.0005$.

4 RESULTS

4.1 Expression of BET reader proteins and c-MYC in EwS

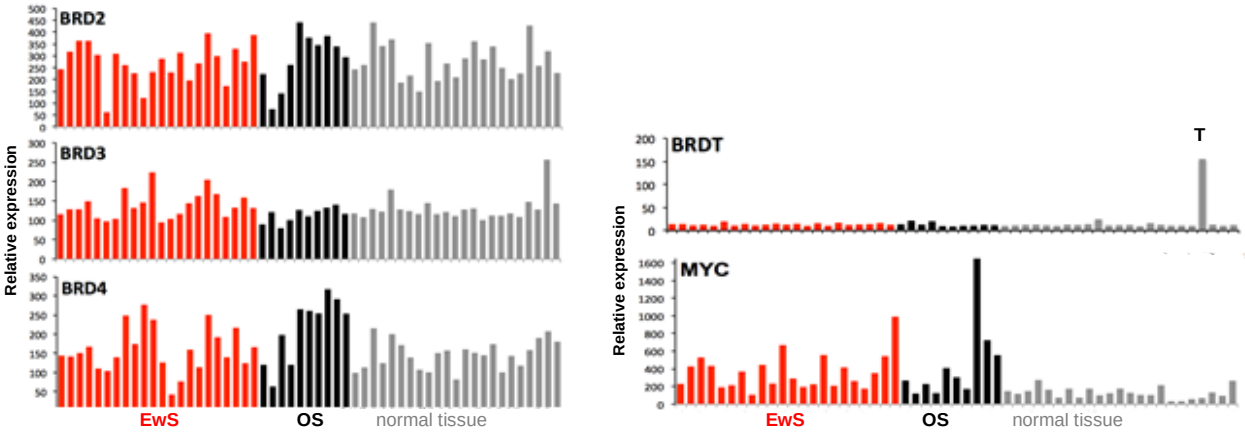

Figure 5: BET and c-MYC expression analysis
Microarray analysis of Ewing sarcoma cell lines (EwS, in red) and Osteosarcoma cell lines (OS, in black) set in relation to normal tissue (in grey) questioning BET and c-MYC transcription expression.

To characterize an EwS specific gene expression profile, EwS tissue was analyzed in a previous microarray study in comparison to normal tissues using high-density DNA microarrays (microarray analysis was performed by Tim Hensel, PhD doctoral candidate). We focused on the expression of BRD2, BRD3, BRD4 and BRDT as well as c-MYC expression and compared it to Ewing Sarcoma (EwS), Osteosarcoma (OS) and normal tissue. **Figure 5** reveals that BRD2, BRD3 and BRD4 are commonly expressed in several normal tissues whereas expression of BRDT only occurs in the testis (T). Interestingly, no significant up- or down-regulation could be observed for BET transcripts in EwS. However, c-MYC showed a significant up-regulation in both EwS and OS in contrast to normal body tissue expression. Therefore, we became curious to find out to which extent the characteristic onco-fusion protein EWS-FLI1 is involved in c-MYC regulation and whether BET bromodomain reader proteins play a key role in EwS performance.

4.2 BET bromodomain family inhibition

Subsequent work demonstrated that mostly cancers driven by specific oncogenic fusions proteins are highly sensitive to epigenetic BET-family inhibition (BETi). To review the observed powerful effect of JQ1, the influence of two other BET

inhibitors, namely I-BET151 (GSK1210151A) and dBET was tested on EwS cell lines. Both avoid the protein-protein interaction between the epigenetic reader proteins of the BET family, acetylated histones and transcription factors by reversibly binding the bromodomain loci of BRD2, BRD3 BRD4 (and BRDT). Previous data demonstrated that inhibition with JQ1 results in significant downregulation of EWS-FLI1 and typical, in EwS normally upregulated and EWS-FLI-dependent genes like *DKK2* (Dickkopf-related protein 2), *GPR64* (G protein-coupled receptor 64), *PAPPA* (Pregnancy-Associated Plasma Protein A, Pappalysin 1), *EZH2* (Enhancer of zeste homolog 2), *STEAP1* (six transmembrane epithelial antigen of the prostate 1) and HOX10 (homeobox-leucine zipper 10). To validate these results, genetic expression on the mRNA level was tested after treatment with I-BET151.

4.2.1 I-BET151 decreases the EwS specific expression profile

I-BET151 inhibits the expression of the typical EwS chimeric fusion gene EWS-FLI1 and alters its specifically expressed epigenetic program. **Figure 6** shows a dose dependent reduction of *EWS/FLI1*, *GPR64* and *PAPPA* in two cell lines A673 and SK-N-MC. Additionally, the expression of *DKK2* is decreased too - but not related to a dose effect - while *c-MYC* is not influenced at all.

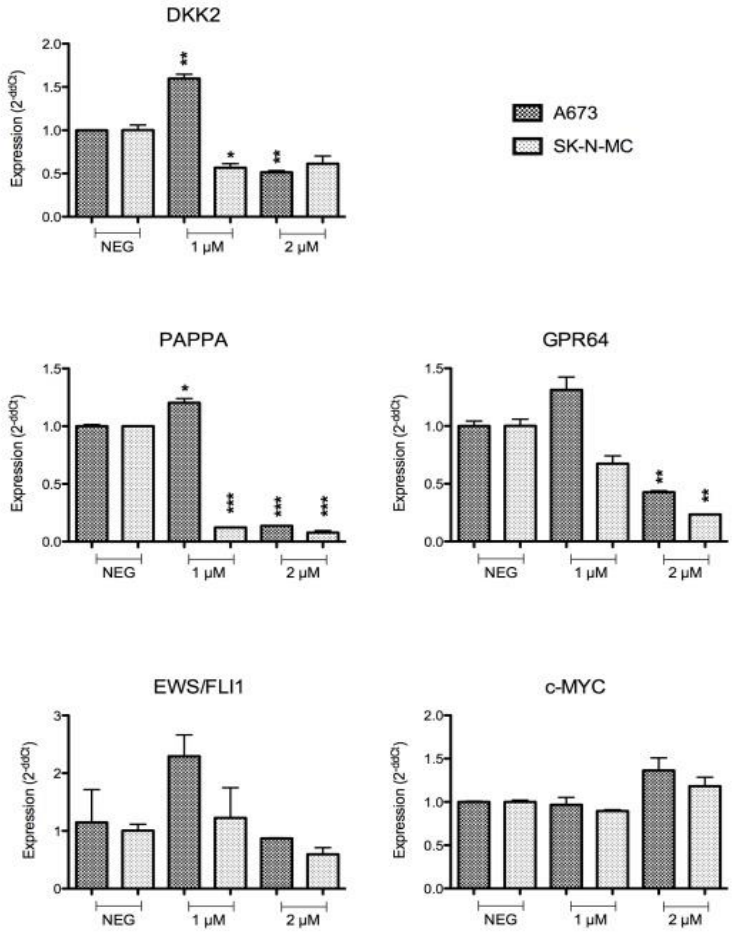

Figure 6: I-BET151 inhibits dose-dependently EwS genomic profile
A673- and SK-N-MC-cells were incubated at 37°C and 5% CO_2 for 48 h with 1 µM or 2 µM I-BET151. Relative expression 2^{-ddCt} was gained by performing qRT-PCR with respective Taq-Man qRT-PCR primers. NEG = cells were treated with equal amount of DMSO which serves as negative controls.
Data are mean ± SEM of two independent experiments; student's t-test (*p < 0.05; **p < 0.005; ***p < 0.0005).

The following assay shown in **Figure 7** includes additional targeted genes after an application of 2 µM for 24 hours. This data confirms the primary results and reveals significantly reduced mRNA expression of important genes in EwS: *EWS/FLI1*, *DKK2*, *PAPPA*, *STEAP1* and *GPR64* were reduced to 5 – 35% in all three cell lines. *EZH2* was decreased only in A673 and SK-N-MC (~50 – 70%). In contrast, *c-MYC* and *HOX 10* were not affected or even up-regulated by the use of I-BET151.

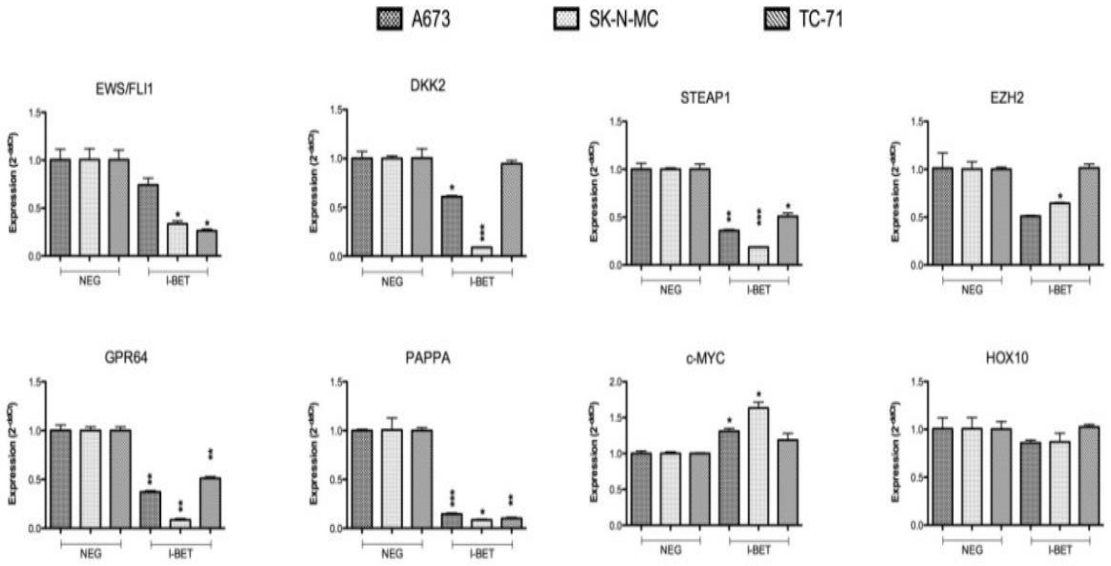

Figure 7: 2 µM I-BET151 decreases further characteristic genes in EwS
After 24 hours RNA was taken, and cDNA was edited, qRT-PCR-assay show significantly reduced expression in three respective cell lines A673, SK-N-MC and TC-71. Data are mean ± SEM of two independent experiments; student's t-test (*p < 0.05; **p < 0.005; ***p < 0.0005).

4.2.2 I-BET151 compared to JQ1

Recently, many investigations have confirmed the powerful anti-tumorous effect of the small molecule JQ1 in several cancers. With the aim of further understanding the BET family protein function for EwS, JQ1 is set in contrast to the resulting effects by I-BET151. The comparisons were made concerning their ability to stem the typical genomic expression profile of EwS. As expected, in the three cell lines A673, SK-N-MC and TC-71 expression levels of target genes are significantly reduced by JQ1 as well as by I-BET151 when compared to the negative control. **Figure 8** presents the data gained by qRT-PCR: 10 different primers (*BRD2*, *BRD3*, *BRD4*, *c-MYC*; *PAPPA*, *GPR64*, *EWS/FLI1*, *DKK2*, *STEAP1* and *EZH2*) were screened after therapeutic treatment.

Consistently, I-BET151 mimics the results measured after JQ1: The members of the BET family *BRD2*, *BRD3* and *BRD4* were not down-regulated, in most cases, their expression stays the same or even increases. In contrast, *PAPPA*, *GPR64* and *STEAP1* are constantly diminished to 5 – 40% genomic expression; meanwhile, *DKK2* and *EZH2* still show a remaining expression between 55 – 80%. I-

BET151 affects the regulation of the EwS oncogenic fusion protein *EWS/FLI1* on average down to 50%, just as well as JQ1.

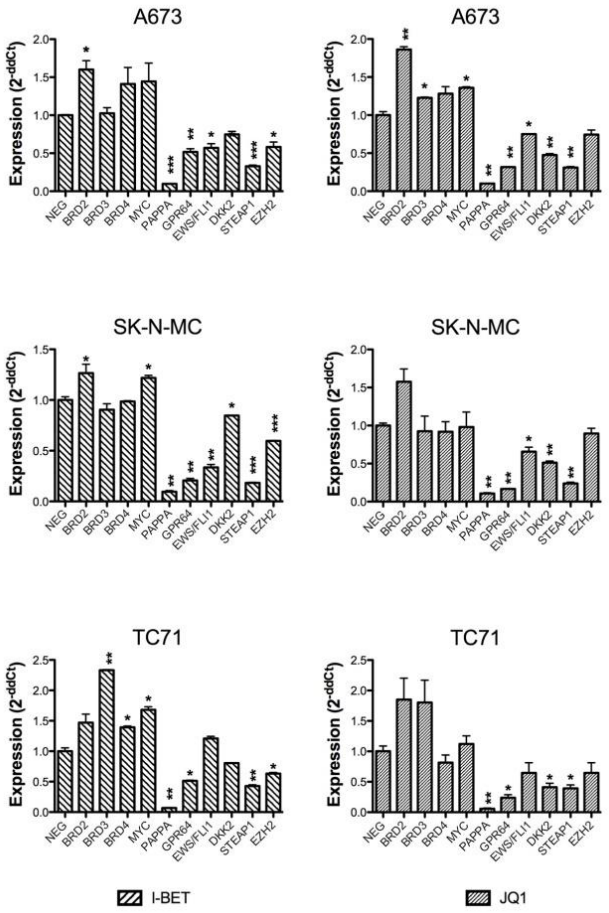

Figure 8: I-BET151 vs. JQ1
Cells were treated 48 h in advance with 2 µM I-BET151, JQ1 or DMSO, which serves as the negative control (NEG). RNA was gained, and compounded cDNA was paired with different typical EwS primers. qRT-PCR was performed. Observations after JQ1 are likewise mimicked by I-BET151 in three cell lines.
Data are mean (of two independent experiments) ± SEM, student's t-test (*$p < 0.05$; **$p < 0.005$; ***$p < 0.0005$).

4.2.3 BET blockade inhibits proliferation in EwS

To primarily investigate the BRD-proteins prominence in EwS viability, the BET inhibitor I-BET151 was used to perform an xCELLigence based proliferation assay. As shown in **Figure 9** the stake of I-BET151 decreases or even prevents the

number of viable cells very significantly in two cell lines A673 and SK-N-MC. Samples were compared to a negative control likewise affected with DMSO (NEG). The proliferation in TC-71 was reduced, too, but did not show significant data.

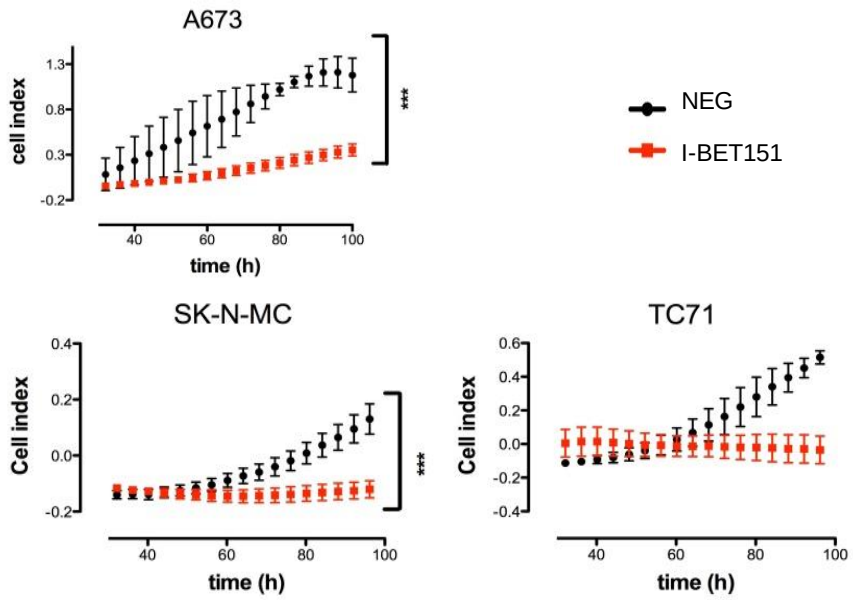

Figure 9: xCELLigence assay performed with 2 µM I-BET151
The cell's impedance (Cell index) was measured every 4 hours. Samples were seeded in hexaplicates per group. In black: negative control with 2 µM DMSO (NEG); In red: inhibiting agent (I-BET151).
Data are mean ± SEM, student's t-test (*p < 0.05; **p < 0.005; ***p < 0.0005).

Additionally, the competitive antagonist of BET bromodomains dBET1 with the ability to attack the cereblon E3 ubiquitin ligase complex was questioned in the same context. This inhibitor leads to selective BET protein degradation and results in a highly delayed progression of the cell lines A673 and SK-N-MC (see **Figure 10**).

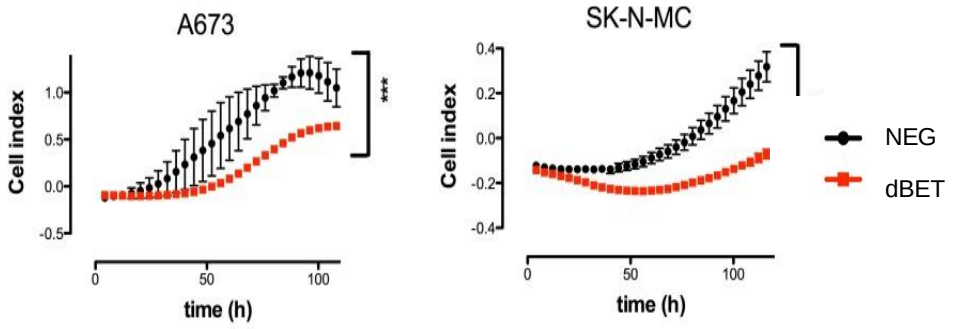

Figure 10: dBET's influence on cell proliferation in EwS
Cell index results out of measured impedance every 4 hours. In black: Negative controls treated with 2 µM DMSO (NEG); in red: The dBET targeted cell lines, also with 2 µM.
Data are mean ± SEM, experiments were done in hexaplicates per group, student's t-test (*p < 0.05; **p < 0.005; ***p < 0.0005).

4.3 The impact of single BET bromodomain reader proteins on EwS

Subsequent data regarding pan-BETi with JQ1 by competitive binding revealed mostly displacement of BRD4 (Filippakopoulos et al., 2010). To further analyze the impact of the single epigenetic BET bromodomain proteins for the tumor's malignancy and to investigate their individual function for EwS, the author of this study established two different knock-down methods with RNA interference (RNAi). Several *in vitro* assays were performed with either transiently (siRNA) or constitutively (shRNA) down-regulated BRD2, BRD3 and BRD4 cell lines (A673, SK-N-MC and TC-71)

4.3.1 Transient knock-down of BET family

Transient knock-down was mediated by three different siRNAs (siBRD2, siBRD3, siBRD4; see **Table 13**: List of siRNA). RNA was taken 48 hours after transfection, cDNA was gained as described in 3.4 and the knock-down efficiency was measured using qRT-PCR with specific TaqMan Primers (see table 0). As **Figure 11** demonstrates, mRNA levels of BRD3 and BRD4 were suppressed in SK-N-MC, A673 and TC-71 down to 10 – 30% after RNAi, while BRD2 knock-down efficiency in A673 and SK-N-MC was only suppressed to 30 – 50% and had no impact in TC-71. Additionally, the corresponding protein analysis for A673 and SK-N-MC performed by Western blot procedure is shown in **Figure 12**: Similar to the qRT-PCR data, the originated BRD protein banner compared to the loading control with the

house keeping protein β-Tubulin (55 kDa) is nearly completely washed out. For both cell lines A673 and SK-N-MC, the knock-down on the protein level after siBRD2 and siBRD4 is strongly effective; the corresponded bands are erased. After siBRD3, the knock-down was highly efficient in A673, but still shows some bindings in SK-N-MC.

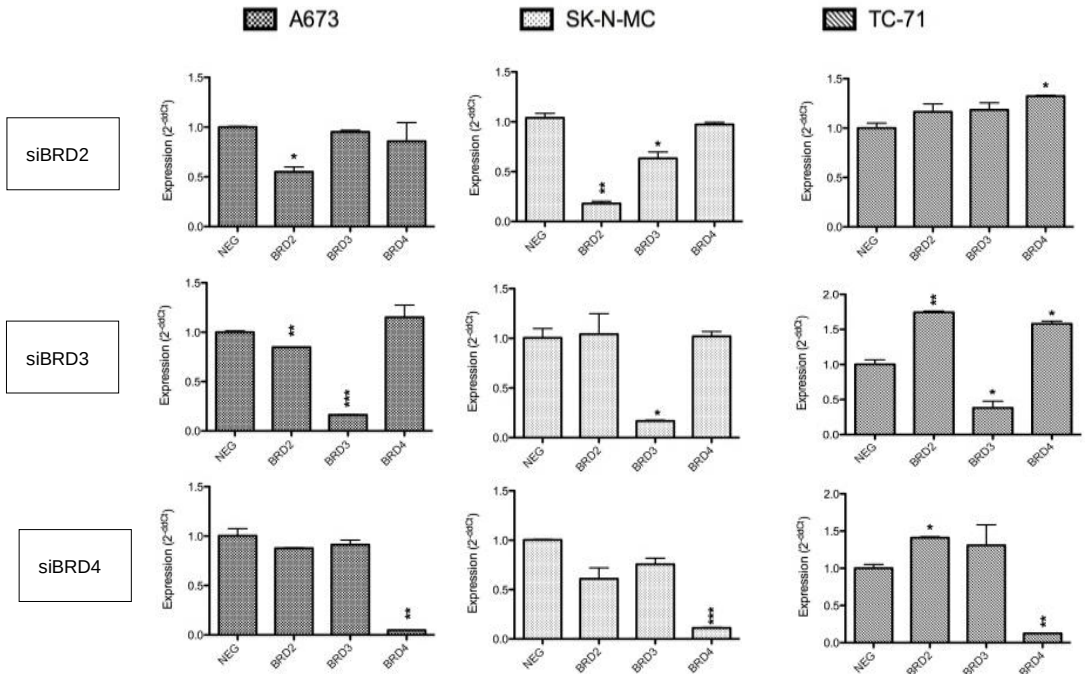

Figure 11: Expression of transient gene knock-down using qRT-PCR
BET bromodomain mRNA levels 48 h after transfection with RNAi with siBRD2, siBRD3- and siBRD4 compared to corresponding negative controls, transfected with non-silencing siRNA (NEG).
Data are mean ± SEM, student's t-test (*p<0.05; **p < 0.005; ***p < 0.0005).
Significantly suppressed samples by BRD4 knock-down were used to perform a microarray analysis (see 4.4).

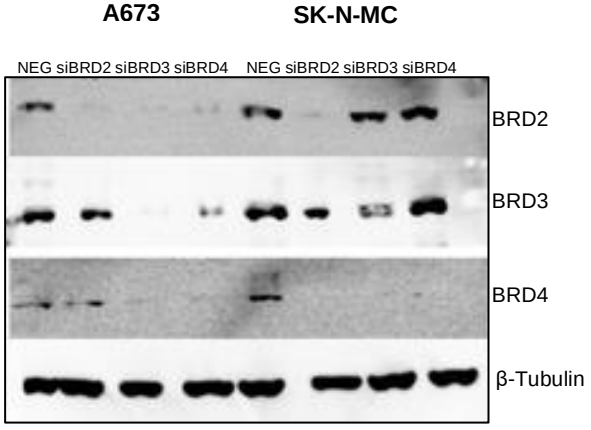

Figure 12: Western Blot analysis after transient gene knock-down with siRNA
Image shows corresponded protein detection after knock-down by WB analysis in comparison to β-Tubulin (55 kDa) in all three cell lines.

4.3.2 Stable genomic silencing of BRD2, BRD3 and BRD4 using shRNA

To permit stable BET family knock-down, three EwS cell lines (A673, SK-N-MC, TC-71) were lentivirally transfected with TRIPZ shRNA. These generated EwS cell lines with constitutive BRD knock-down (shBRD2, shBRD3, shBRD4) permit stable genomic repression mediated by the permanent expression of shRNAs in attendance of doxycycline (Tet-On configuration). This system enables reversible and controlled gene-silencing. The integrated TurboRFP fluorescent reporter allows visual tracking of shRNA expression (see 3.15). Before subsequent functional assays were run RNA was retrieved and minimum levels of remaining gene expression were detected with qRT-PCR (see **Figure 14**). Best effects were observed after 72 hours of induction with doxycycline. In all three cell lines A673, SK-N-MC and TC-71 mRNA levels of BRDs were significantly reduced in a range from 20 – 50% in comparison to cells being transfected with non-silencing shRNA (NEG). Again the corresponding Western blot analysis (house keeping gene: β-Tubulin, 55kDa) is shown in **Figure 13** to verify the knock-down on the protein level.

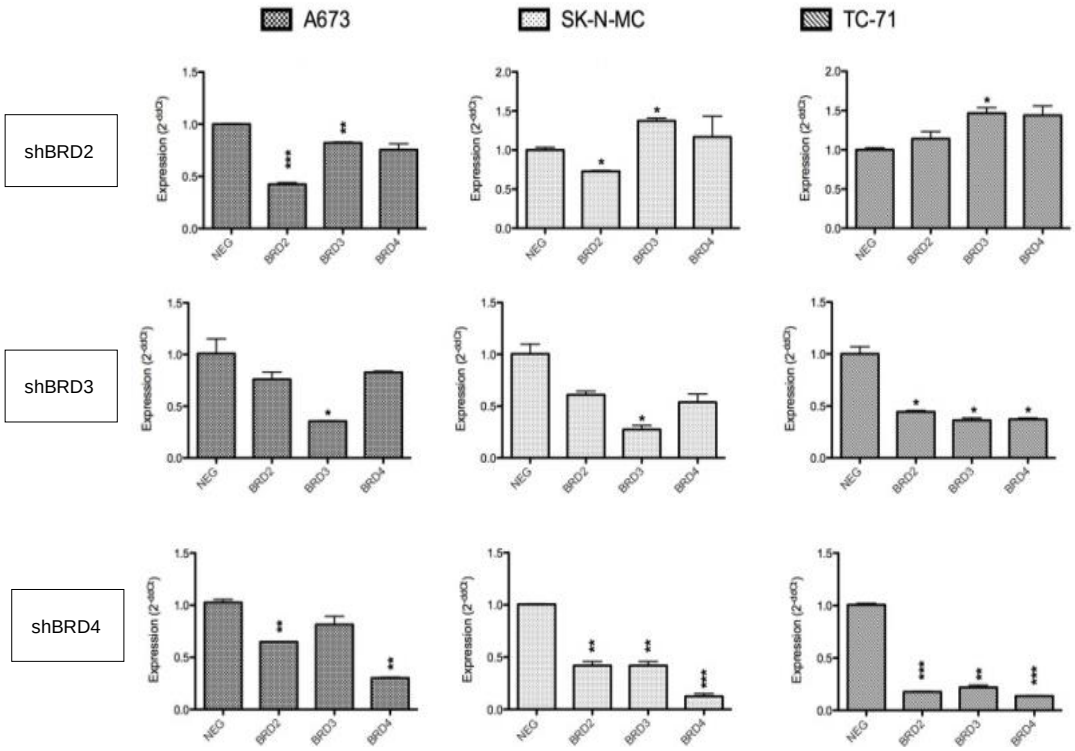

Figure 13: Genomic BRD2, BRD3 and BRD4 expression profile after TRIPZ inducible lentiviral shRNA knock-down
TRIPZ shRNA interference reduced the expression of BRD2, BRD3 and BRD4 mRNA levels due to 72 h induction with 2 µg/ml doxycycline in comparison to non-silencing shRNA control.
Data are mean ± SEM, student's t-test (*p < 0.05; **p < 0.005; ***p < 0.0005).

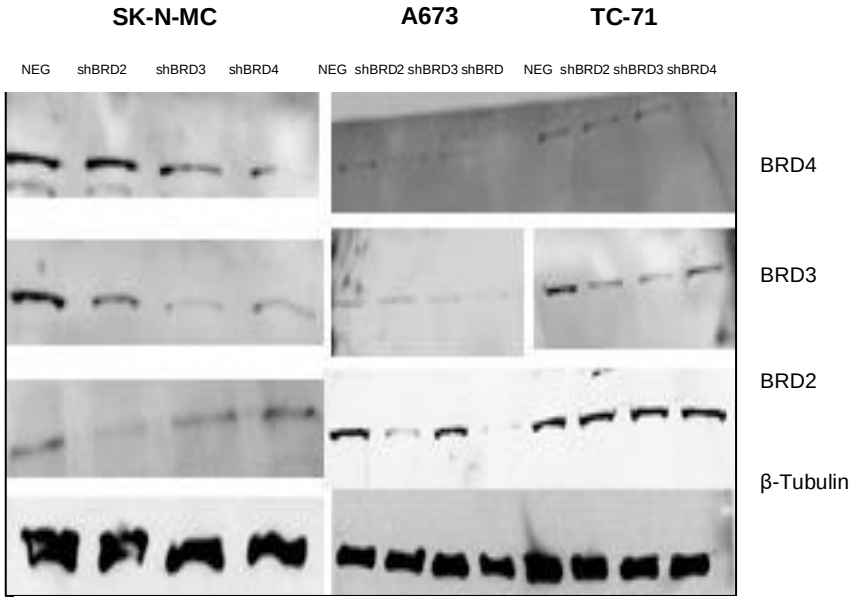

Figure 14: Corresponding Western blot analysis for protein level control after shTRIPZ RNAi
Image shows corresponding protein detection after knock-down by WB analysis in comparison to β-Tubulin (55 kDa) in all three cell lines SKNMC, A673, TC-71.

To examine whether individual BET bromodomain knock-down has a functional influence on the EwS pathogenesis, different in vitro assays were performed with these lentivirally infected TRIPZ shRNA cell lines (A673, SK-N-MC and TC-71).

4.3.3 BRD4 increases proliferation

To analyze the single BRD's influence on the EwS growth pathogenesis, xCELLigence proliferation assays with stable knock-down cell lines were run (see **Figure 15**). Only shBRD4 knock-down significantly inhibits contact dependent growth and results in a decelerated cell proliferation in all three cell lines (particularly obvious statistically significant in A673 and SK-N-MC), whereas RNA interference by shBRD2 and shBRD3 seem to have no impact on the EwS tumor excrescence.

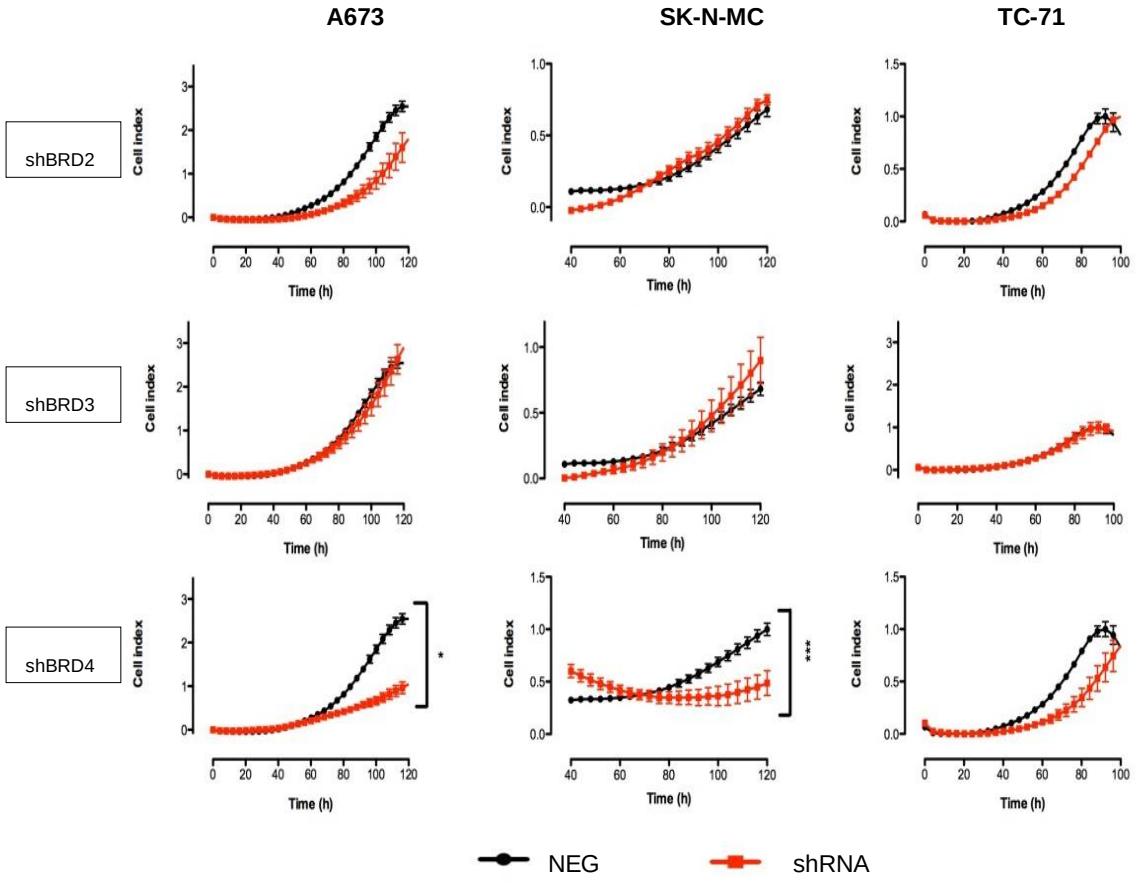

Figure 15: Proliferation assay with constitutively expressed shRNA knock-down repressing genomic expression of BRD2, BRD3 and BRD4
Cell index results out of measured xCELLigence impedance every 4 h. Samples were seeded in hexaplicates per group. In black: negative control with non-silencing shRNA (NEG); red: shBRD knock-down cell line, respectively. Only knock-down of BRD4 inhibits proliferation.
Data are mean ± SEM, student's t-test (*$p < 0.05$; **$p < 0.005$; ***$p < 0.0005$).

4.3.4 BRD4 promotes contact independent growth

The colony forming assay was performed to explore the BRDs' ability to promote contact independent growth into distinct colonies in a semi-solid medium. TRIPZ cells were grown for 14 days at 37°C and 5% CO_2 (see 3.15). For analyzation of grown colonies photos were taken and were enumerated with FIJI imaging systems. Results were compared to negative control cells which are transfected with non-silencing shRNA (NEG). Single knock-down of BRD bromodomain genes results in reduced contact-independent growth capacity in EwS cells *in vitro* (see **Figure 16**). In all TRIPZ cell lines the short hairpin RNA interference of shBRD2, shBRD3 and shBRD4 diminished the cell expansion rate compared to the negative controls at least about 50%. As the performed experiments display, the strongest colony formation inhibition results after shBRD4 most notably in SK-N-MC and TC-71.

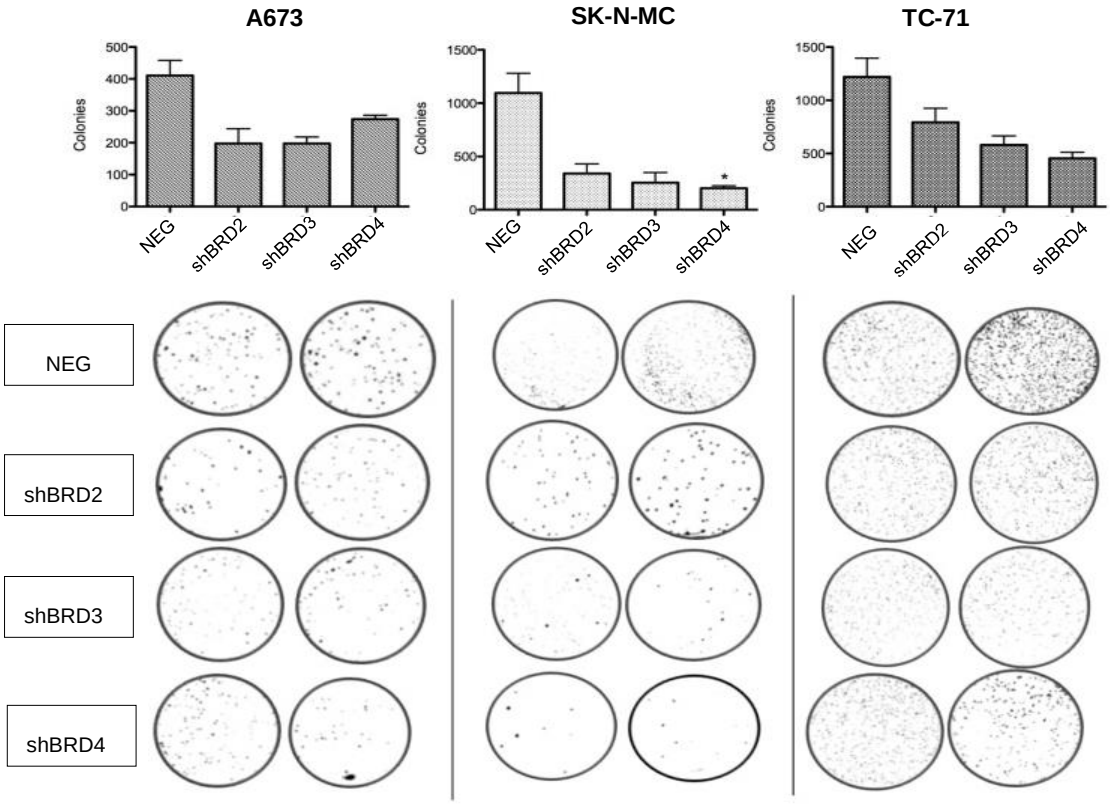

Figure 16: Colony forming assay of constitutive knock-down
Stably transfected shBRD knock-down TRIPZ cell lines A673, SK-N-MC and TC-71 compared to respective non-silenced negative controls (NEG). For colony forming assay cells were seeded in duplicate into a 35 mm plate at a density of 5x103 cells per 1,1 ml methylcellulose-based media and cultured for 14 days in 37°C / 5% CO_2 in a humidified atmosphere and in presence of 1 µg/ml doxycycline. Quantitative evaluation was done by counting colonies in Fiji software. Shown is the average ± SEM; student's t-test (*p < 0.05; **p < 0.005; ***p < 0.0005). Images show representative experiments. Knock-down blocked colony forming SK-N-MC and TC-71 cell lines most obviously after BRD4 knock-down.

4.3.5 BRD4 promotes invasiveness

To shed further light on EwS phenotype and particularly on EwS invasiveness after BRD knock-down another *in vitro* assay investigating the ability of invasive growth was performed (Matrigel-covered transwell assay; BioCoat™ Angiogenesis System; see 3.13). This effort revealed a significantly reduced invasiveness of all three stable transfected shRNA cell lines (see **Figure 17**). Again, the knock-down of BRD4 disclosed the highest impact: In all three stable shRNA knock-down TRIPZ

cell lines A673, SK-N-MC and TC-71 the number of migrated cells through the Matrigel was significantly decreased.

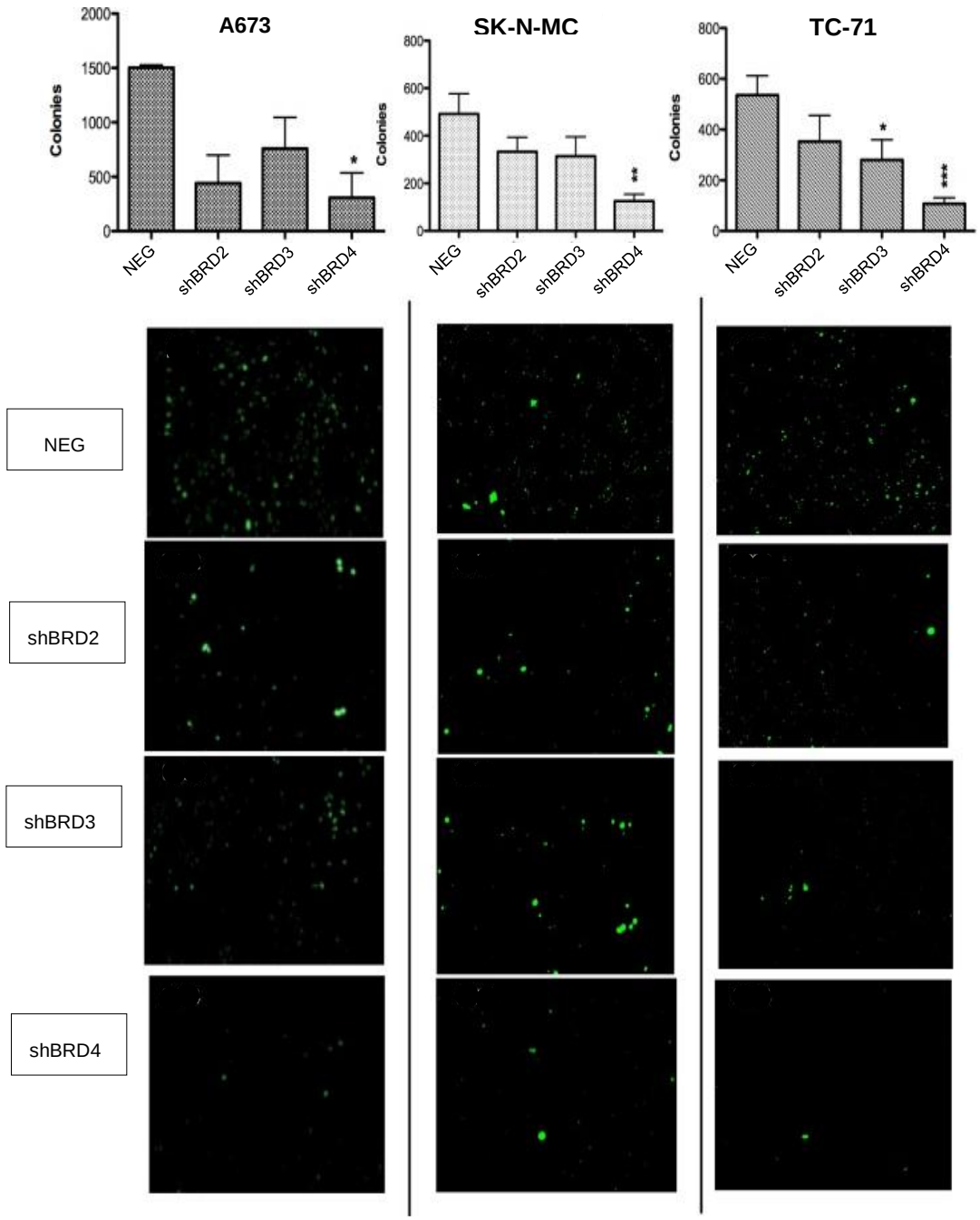

Figure 17: Analysis of invasion of EwS TRIPZ cell lines through Matrigel
Upper panel: Analysis of invasiveness of EwS cell lines through Matrigel after transfection with specific BRD shRNA constructs compared to negative controls with non-silencing shRNA (NEG).
Data are mean ± SEM; student's t-test (*p < 0.05; **p < 0.005; ***p < 0.0005).
Lower panel: Pictures show the performed experiments, respectively. Migrated cells were detected by their resulting fluorescence after staining for 1 hour.

4.3.6 Silencing BRD epigenetic reader proteins alters EwS expression profile

To gain functional insight into how BRD proteins in general and essentially BRD4 influence EwS malignancy several EWS-FLI1 associated or even EWS-FLI1-regulated genes were selected as previously operated with JQ1 and I-BET151. The relative expressions of *c-MYC*, *PAPPA, GPR64*, *STEAP1*, *EZH2*, *EWS/FLI1*, *DKK2, HOX10* and *STK32B* (serine/threonine kinase 32B) were examined with qRT-PCR in three shRNA knock-down cell lines (A673, SK-N-MC and TC-71 with shBRD2, shBRD3 and shBRD4), see **Figure 18**. Overall *PAPPA* and *GPR64* are significantly reduced to 5 – 25% in all cell lines. These genes are thought to be involved in local proliferative processes and in promoting tumor invasion and metastasis. The resulting expression of *DKK2, EZH2* and *HOX10* stays roughly the same (70 – 120%), moreover *STEAP1* and *STK32B* even increase on higher levels. EWS-FLI1 is best affected via shBRD4 in A673. Strikingly, in two cell lines c-*MYC's* expression is reduced (A673 and TC-71). Concluding, besides pan-BETi, also single BRD knock-down leads to alterations of the typical genetic pattern in EwS.

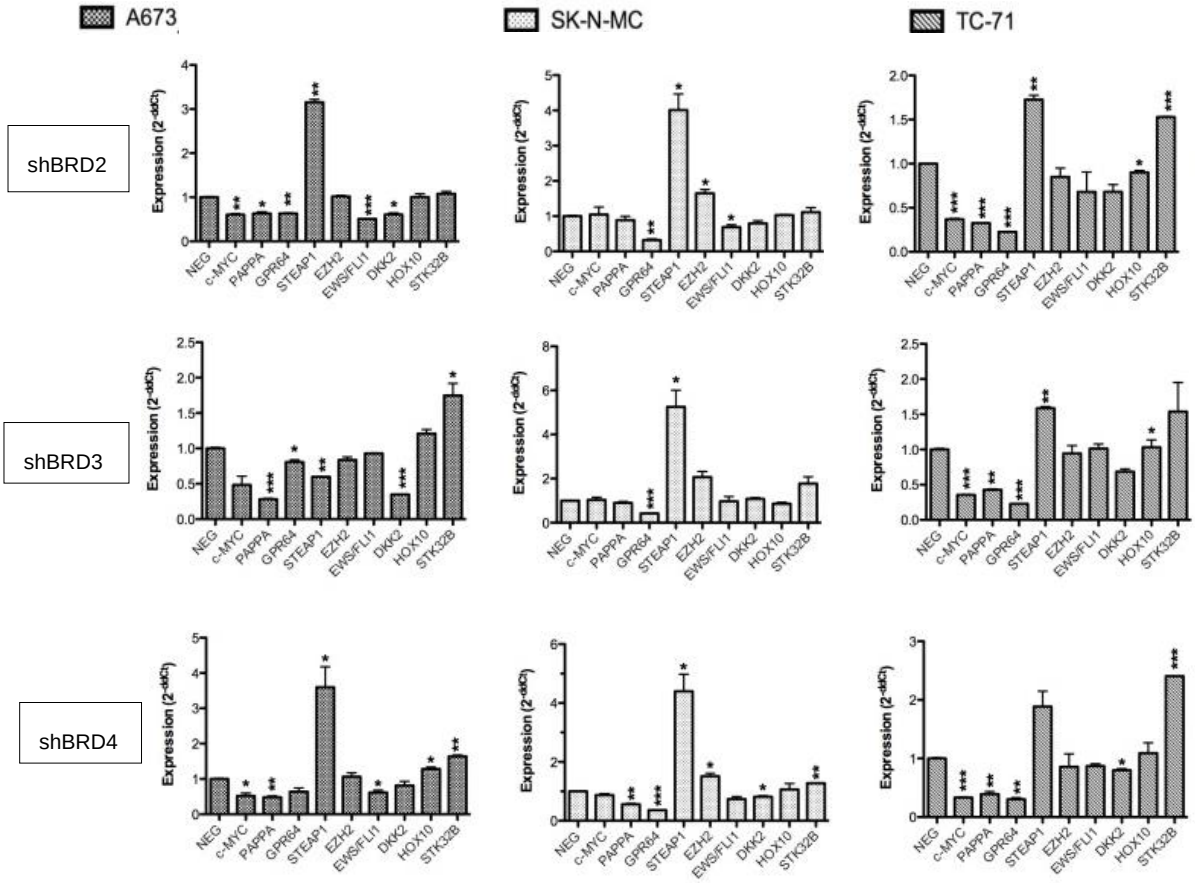

Figure 18: Single BRD knock-down changes genetic pattern in EwS
Image shows reduced mRNA qRT-PCR results after culturing cells 72 h in presence of doxycycline-dependent shRNA. Samples are compared to a negative control. RNA interference of BRD bromodomain family genes downsized expression of EwS/FLI1 and its associated genes, but levels of STEAP1, STK32B and HOX10 did not decrease.
Data are mean ± SEM of two independent experiments; student's t-test (*p < 0.05; **p < 0.005; ***p < 0.0005).

4.3.7 BRD4 RNA interference mimics JQ1 or I-BET151

As demonstrated in 4.3.6 besides effective pan-BETi with small molecules, single knock-down with shRNA decreased the EWS-FLI1 expression and similarly alters its specific expression profile, too. To identify possible major actors and primary objectives within the BET family on mRNA level, we compared these results to data after JQ1 or I-BET151 treatment (see I-BET151 vs. JQ1**Figure 8**). Interestingly, individual genes are equally well down-regulated mostly after constitutive knock-down by siBRD4 or siBRD3 (compare **Figure 19**). Mostly *PAPPA* and *GPR64* are likewise affected and reduced to 20 – 50 %. However, JQ1/I-BET151 treatment did

not show the same effect on *DKK2* expression: SiBRD3 effectively reduced *DKK2* in A673 to 30% and in TC-71 down to 80%. In contrast, pan-BETi affected strongly *STEAP1* in every cell line, but single RNAi only showed a decrease in A673 (siBRD3). All in all, mostly siBRD4 mimicked the anterior results.

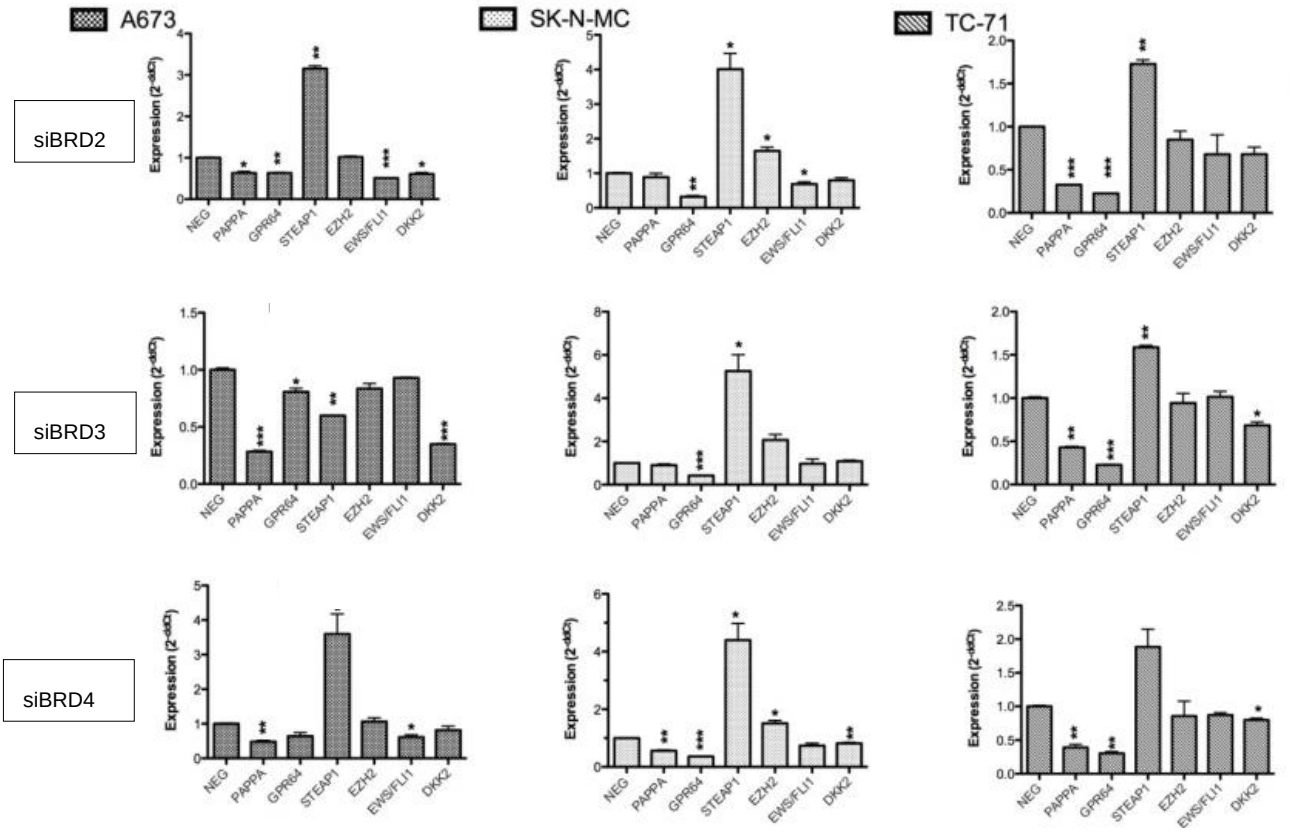

Figure 19: BRD4 imitates JQ1/I-BET151 genomic expression profile
Inducible knock-down cells were cultured 72h in the presence of doxycycline. Samples were compared to non-silencing shRNA (NEG). RNA was isolated and compounded cDNA was paired with different typical EwS primers. qRT-PCR was performed.
Data are mean (of two independent experiments) ± SEM, student's t-test (*p < 0.05; **p < 0.005; ***p < 0.0005).

4.3.8 Individual BRD knock-down does not lead to cell cycle arrest

With the aim to investigate whether RNAi silenced BRD-complexes influence the cell cycle progression, either stable infected shBRD knock-down cell lines (shBRD2, shBRD3, shBRD4) or transient transfected cell lines (siBRD2, siBRD3, siBRD4) were analyzed by flow cytometry. Before cells were assessed in this experiment, RNA was taken, and reduced mRNA levels were confirmed by qRT-PCR to ensure successful knock-down(see 3.7). Therefore, shRNA cell lines were

cultured 72 hours in presence of doxycycline and the cells processed with siRNA were harvested after 48 hours. Then cells were stained with PI (propidium iodide), a nuclear and chromosomal counterstain for cell cycle analysis (see 3.12). Although proliferation of RNAi cells was severely diminished after pan-BET inhibition and by appropriate BRD knock-down (compare 4.2.3 and 4.3.3), this assay gave no doubtless hint on cell cycle alternation or cell cycle arrest: An increase of G1 phase in transient knock-down A673 and SK-N-MC cells and a slight increase of G0/1 phase as well as a reduced mitosis (G2/M) in stable transfected shBRD4 SK-N-MC cell line could be observed (see **Figure 20**), however, no clear differences emerged when compared to the cells transfected with non-silencing shRNA, aside from an increase of the rate of dead cells (~20%). To check whether these gone cells represent either sub-G1 proportions or a significant higher apoptosis rate further tests were run. Respectively, the corresponding cell cycle phase images (FACS analysis) with an increase of the dead cells are shown (**Figure 21**).

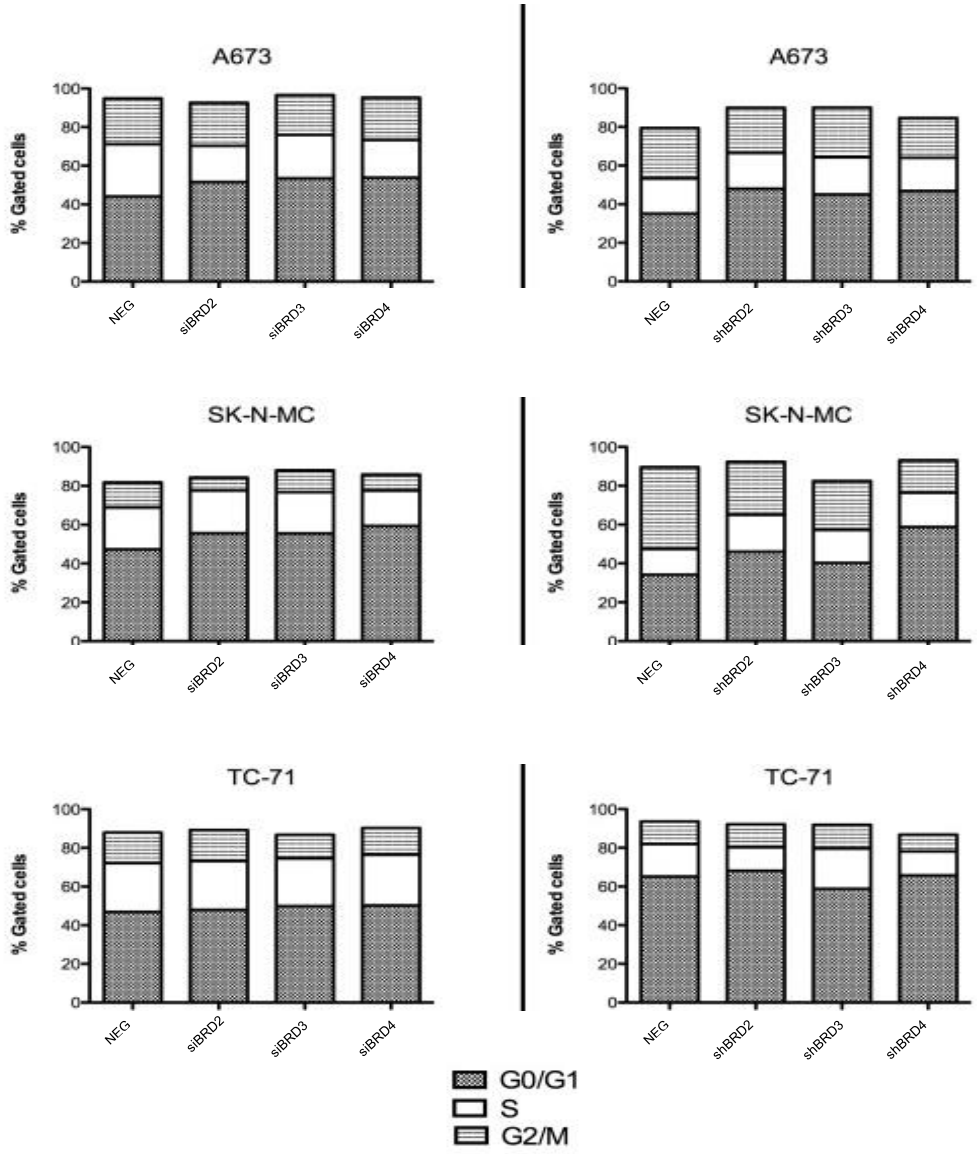

Figure 20: Cell cycle analysis of EwS cell lines after RNAi knock-down (1)
Cell cycle analysis was performed by knocking-down BRD proteins either transient with siRNA (left panel, 48h) or with shRNA (right panel, 72h) compared to negative controls with non-silencing RNAi (NEG). Cells were fixed with ethanol for 16h, stained with propidium Iodide (PI) and analyzed by flow cytometry.

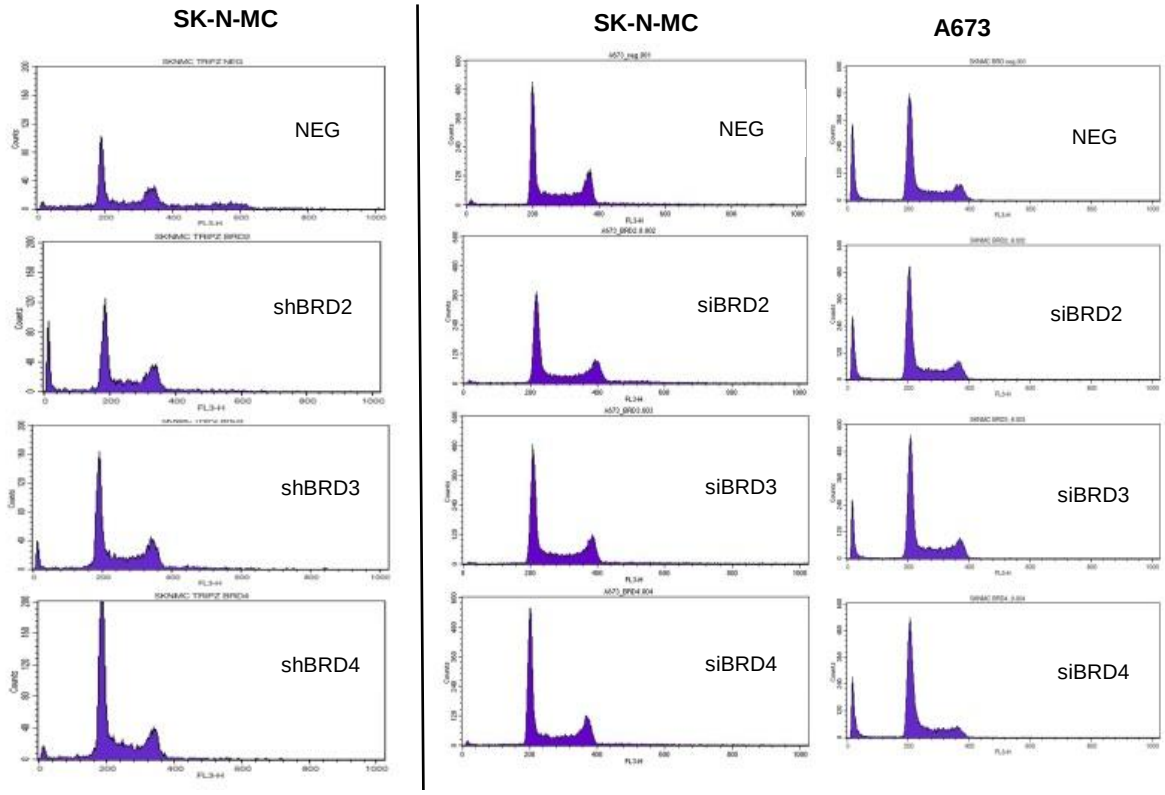

Figure 21: Cell cycle analysis of EwS cell lines after RNAi knock-down (2)
Corresponding representative images of cell cycle analysis with shRNA (left panel) or siRNA transfection (middle and right panel) in SK-N-MC and A673.

4.3.9 Single BRD knock-down does not lead to increased apoptosis

To analyze whether the observed higher rate of dead cells in the FACS analysis could possibly emerge from increased programmed cell death, a Western blot assay was performed with shRNA TRIPZ cell line samples. Two apoptosis biomarkers, namely Casp-7 (Caspase-7) and PARP (Poly-ADP-ribose-polymerase 1), were probed. Caspase-7 is a major executer of initiating apoptosis based on its cleaving capacity. PARP holds an enzymatic function in repairing DNA and is cleaved during apoptosis. Therefore, this method is a very efficient way to detect increased programmed cell death. Only cells with highly effective and statistically significant shRNA-knock-down were used (see **Figure 22**: Apoptosis detection Western blot assays with shRNA cell lines and correspondent rate of knock-down in qRT-PCR**Figure 22**, upper panel). With the extracted proteins from the same probes a Western blot procedure was performed (see **Figure 22**, lower panel). However, no apoptosis activation was found when compared to HPRT as loading control neither after shRBD3 nor shBRD4, concluding that the single members of the BET bromodomain family are not directly involved in apoptosis control.

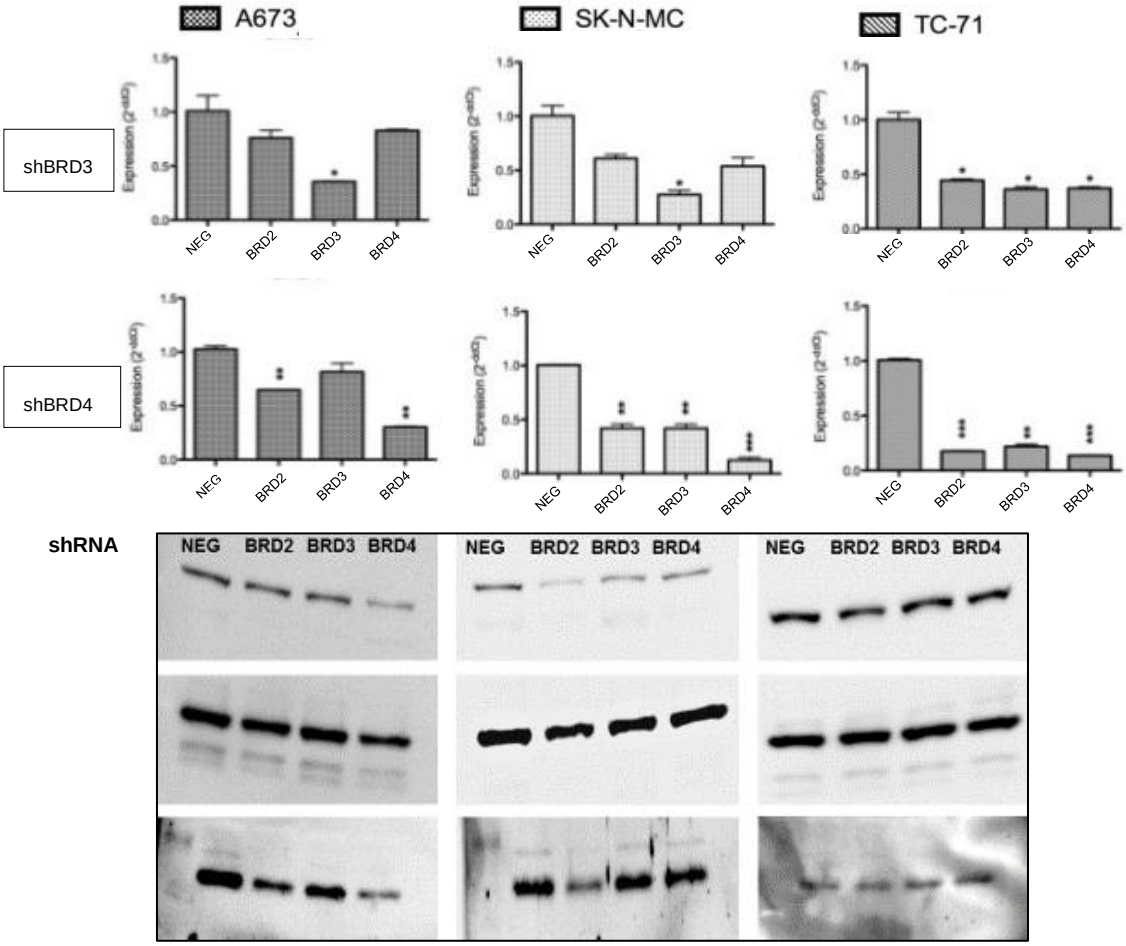

Figure 22: Apoptosis detection Western blot assays with shRNA cell lines and correspondent rate of knock-down in qRT-PCR
Upper panel: Analysis of corresponding appropriate knock-down on mRNA level by RT-PCR. shRNA interference reduced mRNA levels of BRD3 and BRD4 significantly after 72hrs of doxycycline treatment in comparison to non-silencing shRNA control (NEG). Lower panel: Western blot analysis of apoptosis mechanism in three cell lines A673, SK-N-MC and TC-71 after 72h inhibition. Neither shBRD2, shBRD3 or BRD4 lead to cleaved PARP or Caspase-7 (Casp-7).
Data are mean ± SEM, student's t-test (*$p < 0.05$; **$p < 0.005$; ***$p < 0.0005$).

4.4 BRD4 knock-down microarray analysis

To identify up- or down-regulated genes by silencing members of the BET bromodomain gene family a microarray analysis was performed. To highlight to which extend BRD4 inhibition affects gene expression on the transcriptome, samples with significant and reliable BRD4 siRNA knock-down from three cell lines (A673, SK-N-MC, TC-71) were taken and subjected to a whole transcriptome microarray analysis. Microarray data with normalized fluorescent signal intensities were used.

SiBRD4 knock-down in A673 compared to SK-N-MC differentially regulated 562 genes (mean log 1,8-fold change). Previously it was shown that JQ1 inhibits the EWS-FLI1 specific oncogenic fusion protein of EwS and thereby alters the typical EwS expression profile. As the author herein demonstrated, RNAi of BRD4 led to partial mimicry of expression changes after JQ1 inhibition. Thus, to investigate a possible expression overlap with deregulated gene expression after JQ1 treatment, representative siBRD4 knock-down was compared to cells treated with JQ1 in two cell lines (A673 and TC-71): Of 1806 (JQ1) and 1100 (siBRD4) deregulated genes, we found an overlap of 535 genes influenced in both data sets (**Figure 23**, left image). For a Venn diagram, genes ± 1,5 fold differentially expressed were selected for the analysis. The found overlapping deregulated genes also underline the high potential of BRD4's influence on gene expression in EwS.

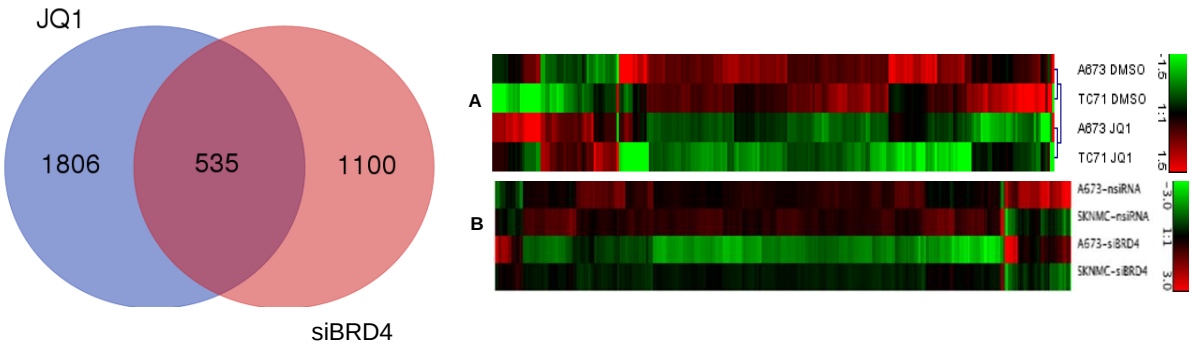

Figure 23: Microarray data
Left: Cells were treated with DMSO or JQ1 for 48 h/siBRD4 for 72h, collected, and then analyzed. For a Venn diagram (http://bioinformatics.psb.ugent.be/webtools/Venn/), genes ± 1,5 fold differentially expressed either after JQ1 treatment or BRD4 knock down were selected for the analysis. **Right**: **A**. Heat map of 244 genes, ±1.8-fold differentially expressed in A673 and TC-71 are shown. **B.** Heat map of 562 genes, ±1,8-fold differentially expressed in 2 different EwS lines A673 and SK-N-MC are shown. Each column represents 1 individual array.

5 DISCUSSION

The typical translocation of Ewing sarcoma (EwS), namely EWS-FLI1, is well known to interfere with normal epigenetic regulation and alters the transcriptional program in terms of maintaining oncogenic transformation (Richter et al., 2009). Tumorigenicity is driven by directly activating or repressing transcription due to enhancer remodeling and creating de-novo super enhancers (Riggi et al., 2014). In cancers, these super-enhancer moieties mostly appear in oncogene-riche regions or interact with genes which are normally involved in cell development and activation of gene expression and cell identity (Whyte et al., 2013). Besides initiating and elongating transcription, these proteins may dispose various other functions like cell cycle regulators or mitotic bookmarks (Doroshow et al., 2017). Yet, directly addressing the exact components in EwS has been challenging: The typical translocation product acts as an aberrant transcription factor. Besides the complicacy of hijacking transcription factors, EWS-FLI1 represents an extra defiance by comprising prion-like domains that can display distinct conformations (Boulay et al., 2017). The fusion product enables specific acetyl-lysine identification marks on histone H3, which are deciphered by epigenetic reader proteins, such as members of the BET family bromodomain proteins BRD2, BRD3 and BRD4 and offer smart options regarding modern medical cancer therapy. In relation to the presented results the author demonstrated the successful inhibition of proliferation with BETi: The findings suggest that the BET family protein members are very promising and reasonable targets for future therapeutics against cancer. Additionally, the performed experiments prove I-BET151 being a well-functioning agonist in comparison to JQ1 based on the suppression of the EwS specific expression profile. Lately, BET inhibition with small molecules such as JQ1 has sparked a new era in anticancer drugs (A. Chaidos et al., 2015; Fu et al., 2015). Furthermore, the author of this study confirmed the high potential of JQ1 in EwS. Subsequent data regarding the deployment of JQ1 has shown efficacy in several types of cancer: other than hematologic malignancies, cancers like adenocarcinoma, neuroblastoma or breast-cancer are effectively treated with single or combined BET inhibition (Mazur et al., 2015; Puissant et al., 2013; Shu et al., 2016). Such inhibition leads to the

reader protein dislodgement from the histone modification and consequently prevents transcription of oncogenic key genes. Interestingly, in nearly all performed *in vitro* experiments with EwS cancer cells BRD4 emerged as the most important submember of the BET family for EwS: BRD4 knock-down led to a significant proliferation stop and revealed the strongest impact on contact-independent growth and invasiveness in EwS. These findings are supported by publications on various tumor types: Herein, only BRD4 deactivation led to delayed tumor progression regarding proliferation, angiogenesis, invasion and cell growths in oral squamous cell carcinoma, HCC, prostate cancer and small cell lung cancer (Bid et al., 2016; Blee et al., 2016; Sun et al., 2016; Wang et al., 2016) (Zhang et al., 2015) (Blee et al., 2016). The author stresses the crucial impact of BRD4 for EwS cancer's development by demonstrating a remarkable suppression of proliferation and invasion.

In EwS's transcriptional program both gene activation and repressing states are present (Riggi et al., 2014). Recent scientific work has demonstrated that BRD4 directly ties to the EWS-FLI1 promotor, recognizing H3K27Ac enlarged binding sites (Jacques et al., 2016). These so-called "super-enhancer" regions are characterized by multiple consecutive GGAA microsatellite repetitions and thereby regulate the transcription of target genes (Gangwal et al., 2008). Epigenetic inhibition of BRD4 by either pan-BET-blockade with small molecules or single BRD genetic knock-down with RNAi results in the inhibition of the typical transcriptional profile of EWS-FLI1 and commutated downstream components: Several – in EwS typically upregulated genes – were found to be likewise downregulated as after treatment with JQ1/I-BET151. Interestingly, mostly BRD4 showed similar effects regarding the strong reduction of *GPR64* and *PAPPA* which may explain the powerful proliferation and invasion restraint after BRD4 silencing. These results are consistent with previous studies in EwS: Richter et al. (Richter et al., 2013) identified the G-protein coupled receptor 64 as the leading driver for promoting invasiveness and metastasis via PGF (placental growth factor) and MMP1 (matrix metalloproteinase 1). Additionally, the pregnancy-associated plasma protein A is known to be involved in local proliferative processes such as wound healing and bone remodeling. Its direct inhibition led to decreased anchorage-dependent and anchorage-independent growth and xenograft cancer formation in EwS (Jayabal et al., 2017). Taken together, this data highlights the essential function of BRD4 within

the EWS-FLI1 altered pathognomonic transcription program for proliferation, invasion and metastasis in EwS.

Vaguely discussed is the influence on c-MYC in EwS after targeting the BRD proteins. The proto-oncogene c-MYC is known to interfere with normal transcriptional activation by modulating global gene expression. Thus c-MYC contributes to tumorigenesis of several tumor entities. Primarily, c-MYC, previously known as one of the most powerful players of cancer pathogenesis, is highly expressed in EwS and OS compared to normal tissue. Genetic variations of c-MYC are often persistently involved in malignant cell proliferation and cancer formation in a variety of oncologic diseases. Recent publications demonstrated that c-MYC is transcriptionally down-regulated after BET inhibition in different malignancies (Coude et al., 2015; Delmore et al., 2011; Ott et al., 2012). Focussing on EwS, a debate is ongoing whether c-MYC and EWS-FLI1 may be connected: Dauphinot et al. demonstrated c-MYC being directly mandated via EWS-FLI1 (Dauphinot et al., 2001). However, other investigations did not show any minimizing influence on c-MYC's expression after treatment with JQ1 in contrast to the genetic expression of EWS-FLI1 (Hensel, Giorgi et al. 2016, Loganathan, Tang et al. 2016). Strikingly, the author of this thesis herein demonstrated, that single BRD knock-down via RNA interference revealed to some extent a significant decrease of c-MYC. This effect may be possibly mandated via indirect or additional mechanisms. It seems likely that by preferential loss of one of the BRD bromodomain proteins - preferably BRD4 - the binding to those earlier named super-enhancers is disabled and results in transcriptional repression of c-MYC. As an alternative, Coude, Braun et al. discuss a concordant effect between BRD2 and BRD4 regarding c-MYC in acute leukemia (Coude et al., 2015). A similar connection between BRD4 and c-MYC was also confirmed in prostate cancer (Loven et al., 2013). However, the underlying mechanisms regarding c-MYC in EwS remain unclear so far and further investigation will be needed to clarify these results.

Even though BRD4 plays the most important role in EwS, a modest decrease in invasion, colony formation and changes of the specific expression pattern were also noticed after BRD2 or BRD3 gene knock-down. Actually, all single BRD proteins target their specific chromatin binding sites but may have overlapping or even

opposing features. Roberts et al. (2017) identified BRD4 as the most potent actor in the regulation of skeletal myogenesis, but they also discuss an oppositional behavior of BRD3 and BRD4 regarding myogenic differentiation. They hypothesize that the association of BRD4 with the genome becomes more specialized upon the initiation of differentiation in contrast to BRD3, which may act later during this process. A reason to consider their concept may be that exclusive inhibition of BRD4 in EwS phenocopied the altered genomic expression of main oncogenic genes in EwS following JQ1 treatment. Remarkably, in this study, single BRD knock-down only partly reproduced the observed effects after JQ1 and I-BET151 treatment. Unfortunately, no clear pattern of the molecular mimicry pattern can be detected. Consequently, it is possible that the questioned targets - which pave the way to a pro-tumorigenic cell state as for instance *GPR64*, *EWS/FLI1*, *DKK2*, *STEAP1* and *EZH2* - are especially needed to promote this process.

Furthermore, a straightforward alliance between EWS-FLI1 and BRD4 was previously observed (Jacques et al., 2016). Basically, BRD4 indirectly facilitates RNA Polymerase II (Pol II) progression via enhanced recruitment of P-TEFb. Active transcription is built upon the phosphorylation of the carboxyl-terminal domain (CTD) of Pol II. The complex formed by BRD4, the P-TEFb subunits CDK9 and Cyclin T1 initiates the phosphorylation of the Ser2 region on RNA polymerase II which prompts the release of paused Pol II in productive transcription elongation genome-wide (Taniguchi, 2016). This kinase regulation by BRD4 has already been proved (Bisgrove, 2007). With regard to the fact that the other members BRD2 and BRD3 ease the Pol II elongation process and inhere an inner histone chaperone-activity or even an autophosphorylation activity, too (LeRoy et al., 2008), a substitution or overlapping effect between the single BRD proteins to regulate transcription and to maintain the EwS tumor’s progression capacity seems likely. Supposedly, all members of the BRD family are of assistance to each other under severe conditions. Interestingly, recent investigations have shown that permanent treatment with JQ1 leads to resistance. Therefore, to circumvent this effect, there is a compelling demand of enhance blockage, either by pan-BET-inhibition and its proteosomal degradation (Dai et al., 2017) or by combination of different agents targeting the transcriptomal process: Some synergistic therapy approaches are already undergoing clinical trials (Kurimchak et al., 2016; Ramadoss & Mahadevan, 2018).

Recent data have shown promising effects against multiple malignancies by including CDK9 inhibition and display an interesting therapeutic strategy (Bacon & D'Orso, 2019). Consequently, a concomitant dual inhibition of BRD4 and CDK9 has revealed an innovative target option and demonstrated a strong inhibition of tumor growth in EwS (Richter et al, submitted).

The fact that BRD4 can form a heterogenous complex with CDK9 and has a role in stimulating productive transcription in EwS is supported by the following observation: The author of this study showed that single BRD knock-down does not lead to increased cell death. The combination of coadjutant BRD family members and the proposal that CDK9 as an antiapoptotic protein can function via BRD4 may explain the lack of increased PARP or Caspase levels in Western blot analysis. However, cell cycle analysis revealed a slight increase in G1 phase exclusively after BRD4 knock-down. These results differ from subsequent findings after JQ1 treatment, which overall resulted in higher alteration of cell cycle regulation and increased apoptosis (Hensel et al., 2016). Besides a complex assembly of different proteins for cell cycle regulation, P-TEFb is known for its activation of growth-associated key genes, governing the course from G1 to early S phase (Yang et al., 2008). With regard to the BRD4-dependency of P-TEFb recruitment, the abrogation of this process by BRD4 RNA interference reduces the activity of efficient bindings and may consequently result in an increased G1 arrest.

In conclusion, the author of this thesis confirms the recent approach of targeting cancer progression by BET inhibition in EwS. Overall, the results state that EWS-FLI1 driven epigenetic phenotype can be successfully addressed by pan-BET inhibition and partially by single BRD knock-down. Moreover, the BRD4’s role as the presumably leading BRD protein family member in EwS regarding tumor proliferation and carcinogenesis is corroborated.

6 SUMMARY

Ewing Sarcomas as highly malignant bone or soft tissue tumors are genetically driven by specific translocation products encoding EWS-ETS proteins, mainly EWS/FLI1. Previous results indicated, that this fusion protein alters the landscape of the epigenetic machinery of normal cells. The epigenetic change of tumor cells does not involve a modification of the nucleotide sequence, but varies the histone structure, e.g. by additional methylations. The resulting chromatin marks are read by so-called “reader-proteins”, who decipher the changed, malignant code and thereby maintain a continuous tumor development. This is done either by chromatin opening and generating super enhancers of prominent oncogenes or by activity loss of tumor suppressors. During the last years different therapeutics with epigenetic effects as a new and safe option for targeted therapy against several malignant diseases became more and more popular. In this study we focused on the BET bromodomain protein family members (BRD2, BRD3 and BRD4), which are overall stably expressed in Ewing Sarcomas. We aimed to investigate their individual role for Ewing sarcoma specific expression profile and malignancy. They consist of amino acid chains that form a hydrophobic pocket to capture acetylated lysine residues on the N-terminal tails of histones to promote fast transcription. We showed that this progress is highly affected by epigenetic blocking: The inhibition of the BET protein family with small molecules like JQ1 or I-BET151 reduced the activity of the specific fusion protein, altered the proper transcriptional expression program and decreased neoplastic development in size, invasiveness and proliferation. Additionally, Ewing sarcomas are also vulnerable to the suppression of single BRD proteins, e. g. by RNA interference. The results resembled the effects after inhibition of the whole reader protein family with small molecules, but it became apparent that BRD4 holds the key function regarding the underlying epigenetic regulation mechanisms for tumorigenesis in Ewing sarcomas. By sufficiently blocking malignant growth, proliferation and invasiveness, BRD4 acts as the most potential BET family member. However, the gained data also depicted that the exclusive blocking of one type of the BET members is not sufficient: Single BRD inhibition only in part resembled the results after the treatment with JQ1 or I-BET151. These findings led us to the hypothesis of a possible reciprocal substitution in case of single BRD loss. Also, supposedly the current discussion about tumor cells developing a resistance after constant long-term treatment, correlates to our observed effects. Hitherto attempts to understand the basic epigenetic machinery in Ewing Sarcomas showed a direct interaction of BRD4 with EWS/FLI1 and possibly

CDK9 and might be efficiently addressed by co-inhibition with other inhibitors, e.g. CDK9 blockers.

7 ZUSAMMENFASSUNG

Ewing Sarkome sind hochmaligne Weichteil- und Knochentumore, die durch spezifische genetische Translokationsprodukte der EWS-ETS-Gruppe induziert werden, allen voran durch EWS/FLI1. Vorherige Ergebnisse zeigten, dass dieses Fusionsprotein die Architektur der epigenetischen Mechanismen normaler Zellen verändert. Die Veränderungen der Tumorzellen beziehen keine Modifikationen der Nukleotidsequenzen ein, sondern variieren die Struktur der Histone, zum Beispiel durch zusätzliche Methylierungen. Die sich hieraus ergebenden Chromatin Markierungen werden von sogenannten „Reader-Proteinen“ gelesen, welche den veränderten, bösartigen Code entziffern und somit die kontinuierliche Ausbildung des Tumors aufrechterhalten. Dies geschieht entweder durch die Auflockerung des Chromatins und neu entstandene Superenhancer von wichtigen Onkogenen, oder durch die Aktivitätsverminderung von Tumorsuppressoren. In den letzten Jahren sind verschiedene Medikamente mit epigenetischer Wirkung als neue und sichere zielgerichtete Therapie gegen viele Krankheiten immer mehr bekannt geworden. In dieser Doktorarbeit haben wir uns auf die BET Bromodomän Proteine (BRD2, BRD3 und BRD4) konzentriert, die dauerhaft im Ewing Sarkom exprimiert werden. Ziel dieser Arbeit ist es, ihre individuelle Rolle für das spezifische Expressionsprofil und die Malignität des Ewing Sarkoms zu untersuchen. Sie bestehen aus Aminosäuren-Ketten, die eine hydrophobe Nische formen, um acetylierte Lysinreste am N-terminalen Ende der Histone zu erfassen und somit die schnelle Transkription fördern. Wir zeigen, dass dieser Ablauf stark durch epigenetische Blockierung beeinflussbar ist: Die Inhibierung der gesamten BET Protein Familie durch niedermolekulare Moleküle wie JQ1 oder I-BET151 verringert die Aktivität des typischen Fusionsproteins EWS/FLI1, bewirkt eine Veränderung des spezifischen Transkriptionsprogrammes und verringert das Größenwachstum, die Invasivität und die Proliferationsrate der Neoplasie. Außerdem sind Ewing Sarkome anfällig für die Suppression einzelner BRD Proteine, z. B. durch RNA Interferenz (RNAi). Die Ergebnisse ähnelten zwar denen nach Hemmung aller BRD Proteine durch niedermolekulare Moleküle, aber es wurde ersichtlich, dass das Protein BRD4 eine Schlüsselfunktion bei den epigenetischen Regulationsmechanismen für die Tumorentwicklung im Ewing Sarkom hat. BRD4 reguliert das Tumorwachstum, die Proliferation und die Invasivität und agiert somit als stärkstes Mitglied der BET Proteinfamilie. Jedoch zeigten die erhobenen Daten auch, dass die alleinige Hemmung von einzelnen BET Typen nicht ausreichend ist: Die Ergebnisse spiegelten nur in Teilen die Ergebnisse wie nach einer Behandlung mit JQ1 oder I-BET151

wieder. Diese Entdeckung führte uns zu der Hypothese einer möglichen gegenseitigen Substitution bei einem einzelnen BRD Protein Verlust. Auch die aktuelle Diskussion über eine Resistenzausbildung der Tumorzellen nach einem längeren Behandlungszeitraum korreliert mit unseren Beobachtungen. Die bisherigen Versuche, die transkriptionellen Abläufe des Ewing Sarkoms besser zu verstehen, zeigten eine direkte Interaktion von BRD4, EWS/FLI1 und möglicherweise CDK9 und könnten durch Ko-Inhibition mit anderen Inhibitoren, z. B. CDK9-Blockern, effizient angegangen werden.

8 APPENDICES

8.1 List of abbreviations

Abbreviation	Full name
APS	Ammonium persulfate
BCP	1-bromo-3-chloropropan
BET	Bromodomain and extra-terminal domain
BETi	BET family inhibition
Bp	Base pairs
BRD	Bromodomain containing protein
Casp-7	Caspase-7
CDK	Cyclin dependent kinases
cDNA	Complimentary DNA
CpG	Cytosine-phosphate-Guanine
DEPC	Diethyl Pyrocarbonate
DKK2	Dickkopf 2
DMEM	Dulbecco's Modified Eagle's Medium
DMSO	Dimethylsulfoxid
DNA	Deoxyribonucleic acid
DNMT	DNA methyltransferase
dNTP	Deoxyribonucleotide triphosphate
Ds	Double stranded
DSMZ	Deutsche Sammlung von Mikroorganismen und Zellkulturen
E2F	Elongation factor 2
EDTA	Ethylene-diamine-tetra-acetic acid
ESFT	Ewing sarcoma family of tumors
esR1	Ewing sarcoma breakpoint region 1
ET	Ewing Tumors
EtBr	Ethidium bromide

EwS	Ewing sarcoma
EWS-FLI1	Specific fusion protein in EwS
EZH1	Enhancer of Zeste, homolog 1
EZH2	Enhancer of Zeste, homolog 2
FBS	Fetal bovine serum
FLI1	Friend leukemia integration 1
Fsrg1	female sterile homeotic-related gene 1
GAPDH	Glyceraldehyde-2-phosphate dehydrogenase
GATA1	Transcription factor
GPR64	G-protein-coupled receptor 64
H3	Histone 3
H3K27ac	Histone 3 lysine 27 acetylation
H3K27me3	Histone 3 lysine 27 trimethylation
H4	Histone4
HBSS	Hank’s Buffered Salt Solution
HCL	Hydrochloride
HDAC	Histone deacetylase
HOX10	Homeobox-leucine zipper 10
HPRT	Hypoxanthin-Guanin-Phosphoribosyltransferase
kDa	Kilo Dalton
$MgCl_2$	Magnesiumchlorid
MM	Mastermix
MMP1	Matrix metalloproteinase 1
mRNA	Messenger RNA
MSC	Mesenchymal stem cell
NEAA	Non-essential amino acids
NEG	Negative control
NF-κB	nuclear factor 'kappa-light-chain-enhancer' of activated B-cells
PAPPA	Pregnancy-Associated Plasma Protein A, Pappalysin 1
PARP	Poly (ADP-ribose)-Polymerase 1

PBS	Phosphate buffered saline
PCR	Polymerase chain reaction
PFA	Paraformaldehyde
PGF	Placental growth factor
PI	Propidium iodide
PNET	peripheral neuroepithelioma/neuroectodermal tumors
pTRIPZ	Lentiviral shRNA transfection
qRT-PCR	Real time quantitative PCR
RelA	Proto-Oncogene, NF-KB Subunit
RFC	Replication factor C
RNA	Ribonucleic acid
RNAi	Ribonucleic acid (RNA) interference
RelA	v-Rel avian reticuloendotheliosis viral oncogene homolog A
RPMI	Roswell Park Memorial Institute Medium
RT	Reverse transcriptase // room temperature
SAM	Significance analysis of microarray
SDS	Sodium Dodecyl Sulfate
SDS-PAGE	SDS polyacrylamide gel electrophoresis
SEM	Standard error of the mean
shRNA	Short hairpin RNA
siRNA	Short interfering RNA
Ss	Single stranded
STEAP1	Six transmembrane epithelial antigen of the prostate 1
TAE	TRIS-Acetate-EDTA-buffer
TBST	Tris-buffered saline Tween 20
TC	T-cell
TEFb	positive transcription elongation factor b
TEMED	N,N,N‘,N‘-Tetramethylethan-1,2-diamin
TRI	Trizol reagent

8.2 List of tables

8.3 List of figures

8.4 Publications

8.4.1 Original articles, peer-reviewed

“Combined Inhibition of Epigenetic Readers and Transcription Initiation Targets the EWS-ETS Transcriptional Program in Ewing Sarcoma”

Günther H.S. Richter, Tim Hensel, Oxana Schmidt, Vadim Saratov, Kristina von Heyking, **Fiona Becker-Dettling,** Carolin Prexler, Hsi-Yu Yen, Katja Steiger, Simone Fulda, Uta Dirksen, Wilko Weichert, Shudong Wang, Stefan Burdach and Beat W. Schäfer.

Published in Cancers (Basel), 02/2020

8.4.2 Congress presentations

Poster: “Inhibition of BET bromodomain proteins in Ewing Sarcoma down regulates their transcriptional program and blocks tumorigenicity and invasiveness”

Fiona A. Becker-Dettling, Tim Hensel, Chiara Giorgi, Oxana Schmidt, Julia Calzada-Wack, Frauke Neff, Beat W. Schäfer, Stefan Burdach, Günther Richter

CTOS (Connective Tissue Oncology Society) Annual Meeting, Lisbon, 09/ 2016

8.4.3 Other contributions

Talk: “Targeting the EWS/ETS transcriptional program by BET bromodomain inhibition in Ewing sarcoma”

Tim Hensel, Chiara Giorgi, **Fiona Becker-Dettling,** Julia Calzada-Wack, Frauke Neff, Thorsten Buch, Oxana Schmidt, Beat W. Schafer, Stefan Burdach, Gunther HS Richter

Deutscher Krebskongress, Berlin, 02/2016

Poster: “Combined targeting of the EWS/ETS transcriptional program and PI3Kpathway inhibition blocks tumorigenicity and increases apoptosis in Ewing sarcoma”

Tim Hensel, Chiara Giorgi, **Fiona Becker-Dettling**, Julia Calzada-Wack, Frauke Neff, Thorsten Buch, Oxana Schmidt, Beat W. Schafer, Stefan Burdach, Gunther HS Richter

Annual Meeting of the American Association for Cancer Research, New Orleans, 04/2016

Poster: “BET bromodomain proteins in Ewing sarcoma regulate a specific transcriptional program, tumorigenicity and apoptosis by interacting with EWS-FLI1 and the positive transcription elongation factor”

Tim Hensel, Chiara Giorgi, **Fiona Becker-Dettling**, Julia Calzada-Wack, Frauke Neff, Thorsten Buch, Oxana Schmidt, Shudong Wang Beat W. Schafer, Stefan Burdach, Gunther HS Richter

New Frontiers in Cancer Research, Cape Town, 01/2017

Poster: “Combined targeting of the EWS/ETS transcriptional program by blocking epigenetic readers and transcription initiation in Ewing sarcoma”

Tim Hensel, Chiara Giorgi, **Fiona Becker-Dettling**, Julia Calzada-Wack, Frauke Neff, Thorsten Buch, Oxana Schmidt, Shudong Wang Beat W. Schafer, Stefan Burdach, Gunther HS Richter

Annual Meeting of the American Association for Cancer Research, Washington D.C., 04/2017

9 References

Arkader, A., Myung, K. S., Stanley, P., & Mascarenhas, L. (2013). Ewing sarcoma of the tibia mimicking fibrous dysplasia. *J Pediatr Orthop B, 22*(3), 222-227. doi:10.1097/BPB.0b013e32834dfe4d

Bacon, C. W., & D'Orso, I. (2019). CDK9: a signaling hub for transcriptional control. *Transcription, 10*(2), 57-75. doi:10.1080/21541264.2018.1523668

Belkina, A. C., & Denis, G. V. (2012). BET domain co-regulators in obesity, inflammation and cancer. *Nat Rev Cancer, 12*(7), 465-477. doi:10.1038/nrc3256

Belkina, A. C., Nikolajczyk, B. S., & Denis, G. V. (2013). BET protein function is required for inflammation: Brd2 genetic disruption and BET inhibitor JQ1 impair mouse macrophage inflammatory responses. *J Immunol, 190*(7), 3670-3678. doi:10.4049/jimmunol.1202838

Berger, S. L., Kouzarides, T., Shiekhattar, R., & Shilatifard, A. (2009). An operational definition of epigenetics. *Genes Dev, 23*(7), 781-783. doi:10.1101/gad.1787609

Bid, H. K., Phelps, D. A., Xaio, L., Guttridge, D. C., Lin, J., London, C., Baker, L. H., Mo, X., & Houghton, P. J. (2016). The Bromodomain BET Inhibitor JQ1 Suppresses Tumor Angiogenesis in Models of Childhood Sarcoma. *Mol Cancer Ther, 15*(5), 1018-1028. doi:10.1158/1535-7163.MCT-15-0567

Blee, A. M., Liu, S., Wang, L., & Huang, H. (2016). BET bromodomain-mediated interaction between ERG and BRD4 promotes prostate cancer cell invasion. *Oncotarget, 7*(25), 38319-38332. doi:10.18632/oncotarget.9513

Bonello, D., Camilleri, F., & Calleja-Agius, J. (2017). Angelman Syndrome: Identification and Management. *Neonatal Netw, 36*(3), 142-151. doi:10.1891/0730-0832.36.3.142

Boulay, G., Sandoval, G. J., Riggi, N., Iyer, S., Buisson, R., Naigles, B., Awad, M. E., Rengarajan, S., Volorio, A., McBride, M. J., Broye, L. C., Zou, L., Stamenkovic, I., Kadoch, C., & Rivera, M. N. (2017). Cancer-Specific Retargeting of BAF Complexes by a Prion-like Domain. *Cell, 171*(1), 163-178 e119. doi:10.1016/j.cell.2017.07.036

Burdach, S., Plehm, S., Unland, R., Dirksen, U., Borkhardt, A., Staege, M. S., Muller-Tidow, C., & Richter, G. H. (2009). Epigenetic maintenance of stemness and malignancy in peripheral neuroectodermal tumors by EZH2. *Cell Cycle, 8*(13), 1991-1996. doi:10.4161/cc.8.13.8929

Burdach, S., Thiel, U., Schoniger, M., Haase, R., Wawer, A., Nathrath, M., Kabisch, H., Urban, C., Laws, H. J., Dirksen, U., Steinborn, M., Dunst, J., Jurgens, H., & Meta, Eicess Study Group. (2010). Total body MRI-governed involved compartment irradiation combined with high-dose

chemotherapy and stem cell rescue improves long-term survival in Ewing tumor patients with multiple primary bone metastases. *Bone Marrow Transplant, 45*(3), 483-489. doi:10.1038/bmt.2009.184

Chaidos, A., Caputo, V., & Karadimitris, A. (2015). Inhibition of bromodomain and extra-terminal proteins (BET) as a potential therapeutic approach in haematological malignancies: emerging preclinical and clinical evidence. *Ther Adv Hematol, 6*(3), 128-141. doi:10.1177/2040620715576662

Chaidos, Aristeidis, Caputo, Valentina, & Karadimitris, Anastasios. (2015). Inhibition of bromodomain and extra-terminal proteins (BET) as a potential therapeutic approach in haematological malignancies: emerging preclinical and clinical evidence. *Therapeutic Advances in Hematology, 6*(3), 128-141. doi:10.1177/2040620715576662

Chapuy, B., McKeown, M. R., Lin, C. Y., Monti, S., Roemer, M. G., Qi, J., Rahl, P. B., Sun, H. H., Yeda, K. T., Doench, J. G., Reichert, E., Kung, A. L., Rodig, S. J., Young, R. A., Shipp, M. A., & Bradner, J. E. (2013). Discovery and characterization of super-enhancer-associated dependencies in diffuse large B cell lymphoma. *Cancer Cell, 24*(6), 777-790. doi:10.1016/j.ccr.2013.11.003

Coude, M. M., Braun, T., Berrou, J., Dupont, M., Bertrand, S., Masse, A., Raffoux, E., Itzykson, R., Delord, M., Riveiro, M. E., Herait, P., Baruchel, A., Dombret, H., & Gardin, C. (2015). BET inhibitor OTX015 targets BRD2 and BRD4 and decreases c-MYC in acute leukemia cells. *Oncotarget, 6*(19), 17698-17712. doi:10.18632/oncotarget.4131

Dai, X., Wang, Z., & Wei, W. (2017). SPOP-mediated degradation of BRD4 dictates cellular sensitivity to BET inhibitors. *Cell Cycle, 16*(24), 2326-2329. doi:10.1080/15384101.2017.1388973

Dauphinot, L., De Oliveira, C., Melot, T., Sevenet, N., Thomas, V., Weissman, B. E., & Delattre, O. (2001). Analysis of the expression of cell cycle regulators in Ewing cell lines: EWS-FLI-1 modulates p57KIP2and c-Myc expression. *Oncogene, 20*(25), 3258-3265. doi:10.1038/sj.onc.1204437

Delattre, O., Zucman, J., Melot, T., Garau, X. S., Zucker, J. M., Lenoir, G. M., Ambros, P. F., Sheer, D., Turc-Carel, C., Triche, T. J., Aurias, A., Thomas, G. (1994). The Ewing family of tumors--a subgroup of small-round-cell tumors defined by specific chimeric transcripts. *N Engl J Med, 331*(5), 294-299. doi:10.1056/NEJM199408043310503

Delmore, J. E., Issa, G. C., Lemieux, M. E., Rahl, P. B., Shi, J., Jacobs, H. M., Kastritis, E., Gilpatrick, T., Paranal, R. M., Qi, J., Chesi, M., Schinzel, A. C., McKeown, M. R., Heffernan, T. P., Vakoc, C. R., Bergsagel, P. L., Ghobrial, I. M., Richardson, P. G., Young, R. A., Hahn, W. C., Anderson, K. C., Kung, A. L., Bradner, J. E., & Mitsiades, C. S. (2011). BET bromodomain inhibition as a therapeutic strategy to target c-Myc. *Cell, 146*(6), 904-917. doi:10.1016/j.cell.2011.08.017

Dhalluin, C., Carlson, J. E., Zeng, L., He, C., Aggarwal, A. K., & Zhou, M. M. (1999). Structure and ligand of a histone acetyltransferase bromodomain. *Nature, 399*(6735), 491-496. doi:10.1038/20974

Doroshow, D. B., Eder, J. P., & LoRusso, P. M. (2017). BET inhibitors: a novel epigenetic approach. *Annals of Oncology, 28*(8), 1776-1787. doi:10.1093/annonc/mdx157

Esiashvili, N., Goodman, M., & Marcus, R. B., Jr. (2008). Changes in incidence and survival of Ewing sarcoma patients over the past 3 decades: Surveillance Epidemiology and End Results data. *J Pediatr Hematol Oncol, 30*(6), 425-430. doi:10.1097/MPH.0b013e31816e22f3

Esteller, M. (2007). Epigenetic gene silencing in cancer: the DNA hypermethylome. *Hum Mol Genet, 16 Spec No 1*, R50-59. doi:10.1093/hmg/ddm018

Ewing, J. (1972). Classics in oncology. Diffuse endothelioma of bone. James Ewing. Proceedings of the New York Pathological Society, 1921. *CA Cancer J Clin, 22*(2), 95-98.

Ferri, E., Petosa, C., & McKenna, C. E. (2016). Bromodomains: Structure, function and pharmacology of inhibition. *Biochem Pharmacol, 106*, 1-18. doi:10.1016/j.bcp.2015.12.005

Filippakopoulos, P., Qi, J., Picaud, S., Shen, Y., Smith, W. B., Fedorov, O., Morse, E. M., Keates, T., Hickman, T. T., Felletar, I., Philpott, M., Munro, S., McKeown, M. R., Wang, Y., Christie, A. L., West, N., Cameron, M. J., Schwartz, B., Heightman, T. D., La Thangue, N., French, C. A., Wiest, O., Kung, A. L., Knapp, S., & Bradner, J. E. (2010). Selective inhibition of BET bromodomains. *Nature, 468*(7327), 1067-1073. doi:10.1038/nature09504

Flores, M., Caram, A., Derrick, E., Reith, J. D., Bancroft, L., & Scherer, K. (2016). Ewing Sarcoma of the Pelvis with an Atypical Radiographic Appearance: A Mimicker of Non-malignant Etiologies. *Cureus, 8*(9), e787. doi:10.7759/cureus.787

Fraga, M. F., Ballestar, E., Paz, M. F., Ropero, S., Setien, F., Ballestar, M. L., Heine-Suner, D., Cigudosa, J. C., Urioste, M., Benitez, J., Boix-Chornet, M., Sanchez-Aguilera, A., Ling, C., Carlsson, E., Poulsen, P., Vaag, A., Stephan, Z., Spector, T. D., Wu, Y. Z., Plass, C., & Esteller, M. (2005). Epigenetic differences arise during the lifetime of monozygotic twins. *Proc Natl Acad Sci U S A, 102*(30), 10604-10609. doi:10.1073/pnas.0500398102

Fu, L. L., Tian, M., Li, X., Li, J. J., Huang, J., Ouyang, L., Zhang, Y., & Liu, B. (2015). Inhibition of BET bromodomains as a therapeutic strategy for cancer drug discovery. *Oncotarget, 6*(8), 5501-5516. doi:10.18632/oncotarget.3551

Gamberi, G., Cocchi, S., Benini, S., Magagnoli, G., Morandi, L., Kreshak, J., Gambarotti, M., Picci, P., Zanella, L., & Alberghini, M. (2011). Molecular diagnosis in Ewing family tumors: the Rizzoli experience--222 consecutive cases in four years. *J Mol Diagn, 13*(3), 313-324. doi:10.1016/j.jmoldx.2011.01.004

Gangwal, K., Sankar, S., Hollenhorst, P. C., Kinsey, M., Haroldsen, S. C., Shah, A. A., Boucher, K. M., Watkins, W. S., Jorde, L. B., Graves, B. J., & Lessnick, S. L. (2008). Microsatellites as EWS/FLI response elements in Ewing's sarcoma. *Proc Natl Acad Sci U S A, 105*(29), 10149-10154. doi:10.1073/pnas.0801073105

Garcia-Aragoncillo, E., Carrillo, J., Lalli, E., Agra, N., Gomez-Lopez, G., Pestana, A., & Alonso, J. (2008). DAX1, a direct target of EWS/FLI1 oncoprotein, is a principal regulator of cell-cycle progression in Ewing's tumor cells. *Oncogene, 27*(46), 6034-6043. doi:10.1038/onc.2008.203

Garnier, J. M., Sharp, P. P., & Burns, C. J. (2014). BET bromodomain inhibitors: a patent review. *Expert Opin Ther Pat, 24*(2), 185-199. doi:10.1517/13543776.2014.859244

Gaspar, N., Hawkins, D. S., Dirksen, U., Lewis, I. J., Ferrari, S., Le Deley, M. C., Kovar, H., Grimer, R., Whelan, J., Claude, L., Delattre, O., Paulussen, M., Picci, P., Sundby Hall, K., van den Berg, H., Ladenstein, R., Michon, J., Hjorth, L., Judson, I., Luksch, R., Bernstein, M. L., Marec-Berard, P., Brennan, B., Craft, A. W., Womer, R. B., Juergens, H., & Oberlin, O. (2015). Ewing Sarcoma: Current Management and Future Approaches Through Collaboration. *J Clin Oncol, 33*(27), 3036-3046. doi:10.1200/JCO.2014.59.5256

Goss, K. L., & Gordon, D. J. (2016). Gene expression signature based screening identifies ribonucleotide reductase as a candidate therapeutic target in Ewing sarcoma. *Oncotarget, 7*(39), 63003-63019. doi:10.18632/oncotarget.11416

Greschik, H., Schule, R., & Gunther, T. (2017). Selective targeting of epigenetic reader domains. *Expert Opin Drug Discov, 12*(5), 449-463. doi:10.1080/17460441.2017.1303474

Grunewald, T. G., Diebold, I., Esposito, I., Plehm, S., Hauer, K., Thiel, U., da Silva-Buttkus, P., Neff, F., Unland, R., Muller-Tidow, C., Zobywalski, C., Lohrig, K., Lewandrowski, U., Sickmann, A., Prazeres da Costa, O., Gorlach, A., Cossarizza, A., Butt, E., Richter, G. H., & Burdach, S. (2012). STEAP1 is associated with the invasive and oxidative stress phenotype of Ewing tumors. *Mol Cancer Res, 10*(1), 52-65. doi:10.1158/1541-7786.MCR-11-0524

Grunewald, T. G., Willier, S., Janik, D., Unland, R., Reiss, C., Prazeres da Costa, O., Buch, T., Dirksen, U., Richter, G. H., Neff, F., Burdach, S., & Butt, E. (2013). The Zyxin-related protein thyroid receptor interacting protein 6

(TRIP6) is overexpressed in Ewing's sarcoma and promotes migration, invasion and cell growth. *Biol Cell, 105*(11), 535-547. doi:10.1111/boc.201300041

Gustafson, W. C., & Weiss, W. A. (2010). Myc proteins as therapeutic targets. *Oncogene, 29*(9), 1249-1259. doi:10.1038/onc.2009.512

Hensel, T., Giorgi, C., Schmidt, O., Calzada-Wack, J., Neff, F., Buch, T., Niggli, F. K., Schafer, B. W., Burdach, S., & Richter, G. H. (2016). Targeting the EWS-ETS transcriptional program by BET bromodomain inhibition in Ewing sarcoma. *Oncotarget, 7*(2), 1451-1463. doi:10.18632/oncotarget.6385

Huang, B., Yang, X. D., Zhou, M. M., Ozato, K., & Chen, L. F. (2009). Brd4 coactivates transcriptional activation of NF-kappaB via specific binding to acetylated RelA. *Mol Cell Biol, 29*(5), 1375-1387. doi:10.1128/MCB.01365-08

Jacques, C., Lamoureux, F., Baud'huin, M., Rodriguez Calleja, L., Quillard, T., Amiaud, J., Tirode, F., Redini, F., Bradner, J. E., Heymann, D., & Ory, B. (2016). Targeting the epigenetic readers in Ewing sarcoma inhibits the oncogenic transcription factor EWS/Fli1. *Oncotarget, 7*(17), 24125-24140. doi:10.18632/oncotarget.8214

Jang, M. K., Mochizuki, K., Zhou, M., Jeong, H. S., Brady, J. N., & Ozato, K. (2005). The bromodomain protein Brd4 is a positive regulatory component of P-TEFb and stimulates RNA polymerase II-dependent transcription. *Mol Cell, 19*(4), 523-534. doi:10.1016/j.molcel.2005.06.027

Javaheri, T., Kazemi, Z., Pencik, J., Pham, H. T., Kauer, M., Noorizadeh, R., Sax, B., Nivarthi, H., Schlederer, M., Maurer, B., Hofbauer, M., Aryee, D. N., Wiedner, M., Tomazou, E. M., Logan, M., Hartmann, C., Tuckermann, J. P., Kenner, L., Mikula, M., Dolznig, H., Uren, A., Richter, G. H., Grebien, F., Kovar, H., & Moriggl, R. (2016). Increased survival and cell cycle progression pathways are required for EWS/FLI1-induced malignant transformation. *Cell Death Dis, 7*(10), e2419. doi:10.1038/cddis.2016.268

Jayabal, P., Houghton, P. J., & Shiio, Y. (2017). EWS-FLI-1 creates a cell surface microenvironment conducive to IGF signaling by inducing pappalysin-1. *Genes Cancer, 8*(11-12), 762-770. doi:10.18632/genesandcancer.159

Junwei, Shi, & Vakoc, Christopher R. (2014). The mechanisms behind the therapeutic activity of BET bromodomain inhibition. *Molecular Cell, 54*(5), 728-736. doi:10.1016/j.molcel.2014.05.016

Kennedy, A. L., Vallurupalli, M., Chen, L., Crompton, B., Cowley, G., Vazquez, F., Weir, B. A., Tsherniak, A., Parasuraman, S., Kim, S., Alexe, G., & Stegmaier, K. (2015). Functional, chemical genomic, and super-enhancer screening identify sensitivity to cyclin D1/CDK4 pathway inhibition in Ewing sarcoma. *Oncotarget, 6*(30), 30178-30193. doi:10.18632/oncotarget.4903

Khanna, N., Pandey, A., & Bajpai, J. (2017). Metastatic Ewing's Sarcoma: Revisiting the "Evidence on the Fence". *Indian J Med Paediatr Oncol, 38*(2), 173-181. doi:10.4103/ijmpo.ijmpo_24_17

Khoury, Joseph D. (2005). Ewing Sarcoma Family of Tumors. *Advances in Anatomic Pathology, 12*(4), 212-220.

Kovar, H. (2014). Blocking the road, stopping the engine or killing the driver? Advances in targeting EWS/FLI-1 fusion in Ewing sarcoma as novel therapy. *Expert Opin Ther Targets, 18*(11), 1315-1328. doi:10.1517/14728222.2014.947963

Kurimchak, A. M., Shelton, C., Duncan, K. E., Johnson, K. J., Brown, J., O'Brien, S., Gabbasov, R., Fink, L. S., Li, Y., Lounsbury, N., Abou-Gharbia, M., Childers, W. E., Connolly, D. C., Chernoff, J., Peterson, J. R., & Duncan, J. S. (2016). Resistance to BET Bromodomain Inhibitors Is Mediated by Kinome Reprogramming in Ovarian Cancer. *Cell Rep, 16*(5), 1273-1286. doi:10.1016/j.celrep.2016.06.091

Lamonica, J. M., Deng, W., Kadauke, S., Campbell, A. E., Gamsjaeger, R., Wang, H., Cheng, Y., Billin, A. N., Hardison, R. C., Mackay, J. P., & Blobel, G. A. (2011). Bromodomain protein Brd3 associates with acetylated GATA1 to promote its chromatin occupancy at erythroid target genes. *Proc Natl Acad Sci U S A, 108*(22), E159-168. doi:10.1073/pnas.1102140108

LeRoy, G., Rickards, B., & Flint, S. J. (2008). The double bromodomain proteins Brd2 and Brd3 couple histone acetylation to transcription. *Mol Cell, 30*(1), 51-60. doi:10.1016/j.molcel.2008.01.018

Lessnick, S. L., & Ladanyi, M. (2012). Molecular pathogenesis of Ewing sarcoma: new therapeutic and transcriptional targets. *Annu Rev Pathol, 7*, 145-159. doi:10.1146/annurev-pathol-011110-130237

Loganathan, S. N., Tang, N., Fleming, J. T., Ma, Y., Guo, Y., Borinstein, S. C., Chiang, C., & Wang, J. (2016). BET bromodomain inhibitors suppress EWS-FLI1-dependent transcription and the IGF1 autocrine mechanism in Ewing sarcoma. *Oncotarget, 7*(28), 43504-43517. doi:10.18632/oncotarget.9762

Loven, J., Hoke, H. A., Lin, C. Y., Lau, A., Orlando, D. A., Vakoc, C. R., Bradner, J. E., Lee, T. I., & Young, R. A. (2013). Selective inhibition of tumor oncogenes by disruption of super-enhancers. *Cell, 153*(2), 320-334. doi:10.1016/j.cell.2013.03.036

Lu, Jing, Qian, Yimin, Altieri, Martha, Dong, Hanqing, Wang, Jing, Raina, Kanak, Hines, John, Winkler, James D, Crew, Andrew P, Coleman, Kevin, & Crews, Craig M. (2015). Hijacking the E3 Ubiquitin Ligase Cereblon to Efficiently Target BRD4. *Chemistry & Biology, 22*(6), 755-763. doi:http://dx.doi.org/10.1016/j.chembiol.2015.05.009

Maruyama, T., Farina, A., Dey, A., Cheong, J., Bermudez, V. P., Tamura, T., Sciortino, S., Shuman, J., Hurwitz, J., & Ozato, K. (2002). A Mammalian bromodomain protein, brd4, interacts with replication factor C and inhibits progression to S phase. *Mol Cell Biol, 22*(18), 6509-6520.

Maygarden, S. J., Askin, F. B., Siegal, G. P., Gilula, L. A., Schoppe, J., Foulkes, M., Kissane, J. M., & Nesbit, M. (1993). Ewing sarcoma of bone in infants and toddlers. A clinicopathologic report from the Intergroup Ewing's Study. *Cancer, 71*(6), 2109-2118.

Mazur, P. K., Herner, A., Mello, S. S., Wirth, M., Hausmann, S., Sanchez-Rivera, F. J., Lofgren, S. M., Kuschma, T., Hahn, S. A., Vangala, D., Trajkovic-Arsic, M., Gupta, A., Heid, I., Noel, P. B., Braren, R., Erkan, M., Kleeff, J., Sipos, B., Sayles, L. C., Heikenwalder, M., Hessmann, E., Ellenrieder, V., Esposito, I., Jacks, T., Bradner, J. E., Khatri, P., Sweet-Cordero, E. A., Attardi, L. D., Schmid, R. M., Schneider, G., Sage, J., & Siveke, J. T. (2015). Combined inhibition of BET family proteins and histone deacetylases as a potential epigenetics-based therapy for pancreatic ductal adenocarcinoma. *Nat Med, 21*(10), 1163-1171. doi:10.1038/nm.3952

McCabe, M. T., Ott, H. M., Ganji, G., Korenchuk, S., Thompson, C., Van Aller, G. S., Liu, Y., Graves, A. P., Della Pietra, A., 3rd, Diaz, E., LaFrance, L. V., Mellinger, M., Duquenne, C., Tian, X., Kruger, R. G., McHugh, C. F., Brandt, M., Miller, W. H., Dhanak, D., Verma, S. K., Tummino, P. J., & Creasy, C. L. (2012). EZH2 inhibition as a therapeutic strategy for lymphoma with EZH2-activating mutations. *Nature, 492*(7427), 108-112. doi:10.1038/nature11606

Muller, S., Filippakopoulos, P., & Knapp, S. (2011). Bromodomains as therapeutic targets. *Expert Rev Mol Med, 13*, e29. doi:10.1017/S1462399411001992

Musselman, C. A., Lalonde, M. E., Cote, J., & Kutateladze, T. G. (2012). Perceiving the epigenetic landscape through histone readers. *Nat Struct Mol Biol, 19*(12), 1218-1227. doi:10.1038/nsmb.2436

Nakamura, Y., Umehara, T., Nakano, K., Jang, M. K., Shirouzu, M., Morita, S., Uda-Tochio, H., Hamana, H., Terada, T., Adachi, N., Matsumoto, T., Tanaka, A., Horikoshi, M., Ozato, K., Padmanabhan, B., & Yokoyama, S. (2007). Crystal structure of the human BRD2 bromodomain: insights into dimerization and recognition of acetylated histone H4. *J Biol Chem, 282*(6), 4193-4201. doi:10.1074/jbc.M605971200

Ng, K. P., Cheung, F., & Lee, K. A. (2010). A transcription assay for EWS oncoproteins in Xenopus oocytes. *Protein Cell, 1*(10), 927-934. doi:10.1007/s13238-010-0114-y

Nicodeme, Edwige, Jeffrey, Kate L., Schaefer, Uwe, Beinke, Soren, Dewell, Scott, Chung, Chun-wa, Chandwani, Rohit, Marazzi, Ivan, Wilson, Paul,

Coste, Hervé, White, Julia, Kirilovsky, Jorge, Lora, Jose M., Prinjha, Rab K., Lee, Kevin, & Tarakhovsky, Alexander. (2010). Suppression of inflammation by a synthetic histone mimic. *Nature, 468*(7327), 1119-1123. doi:10.1038/nature09589

Ntranos, A., & Casaccia, P. (2016). Bromodomains: Translating the words of lysine acetylation into myelin injury and repair. *Neurosci Lett, 625*, 4-10. doi:10.1016/j.neulet.2015.10.015

Ott, C. J., Kopp, N., Bird, L., Paranal, R. M., Qi, J., Bowman, T., Rodig, S. J., Kung, A. L., Bradner, J. E., & Weinstock, D. M. (2012). BET bromodomain inhibition targets both c-Myc and IL7R in high-risk acute lymphoblastic leukemia. *Blood, 120*(14), 2843-2852. doi:10.1182/blood-2012-02-413021

Padmanabhan, B., Mathur, S., Manjula, R., & Tripathi, S. (2016). Bromodomain and extra-terminal (BET) family proteins: New therapeutic targets in major diseases. *J Biosci, 41*(2), 295-311.

Perez-Salvia, M., Simo-Riudalbas, L., Llinas-Arias, P., Roa, L., Setien, F., Soler, M., Castro de Moura, M., Bradner, J. E., Gonzalez-Suarez, E., Moutinho, C., & Esteller, M. (2017). Bromodomain inhibition shows antitumoral activity in mice and human luminal breast cancer. *Oncotarget*. doi:10.18632/oncotarget.18255

Puissant, A., Frumm, S. M., Alexe, G., Bassil, C. F., Qi, J., Chanthery, Y. H., Nekritz, E. A., Zeid, R., Gustafson, W. C., Greninger, P., Garnett, M. J., McDermott, U., Benes, C. H., Kung, A. L., Weiss, W. A., Bradner, J. E., & Stegmaier, K. (2013). Targeting MYCN in neuroblastoma by BET bromodomain inhibition. *Cancer Discov, 3*(3), 308-323. doi:10.1158/2159-8290.CD-12-0418

Ramadoss, M., & Mahadevan, V. (2018). Targeting the cancer epigenome: synergistic therapy with bromodomain inhibitors. *Drug Discov Today, 23*(1), 76-89. doi:10.1016/j.drudis.2017.09.011

Richter, G. H., Fasan, A., Hauer, K., Grunewald, T. G., Berns, C., Rossler, S., Naumann, I., Staege, M. S., Fulda, S., Esposito, I., & Burdach, S. (2013). G-Protein coupled receptor 64 promotes invasiveness and metastasis in Ewing sarcomas through PGF and MMP1. *J Pathol, 230*(1), 70-81. doi:10.1002/path.4170

Richter, G. H., Plehm, S., Fasan, A., Rossler, S., Unland, R., Bennani-Baiti, I. M., Hotfilder, M., Lowel, D., von Luettichau, I., Mossbrugger, I., Quintanilla-Martinez, L., Kovar, H., Staege, M. S., Muller-Tidow, C., & Burdach, S. (2009). EZH2 is a mediator of EWS/FLI1 driven tumor growth and metastasis blocking endothelial and neuro-ectodermal differentiation. *Proc Natl Acad Sci U S A, 106*(13), 5324-5329. doi:10.1073/pnas.0810759106

Riggi, N., Knoechel, B., Gillespie, S. M., Rheinbay, E., Boulay, G., Suva, M. L., Rossetti, N. E., Boonseng, W. E., Oksuz, O., Cook, E. B., Formey, A.,

Patel, A., Gymrek, M., Thapar, V., Deshpande, V., Ting, D. T., Hornicek, F. J., Nielsen, G. P., Stamenkovic, I., Aryee, M. J., Bernstein, B. E., & Rivera, M. N. (2014). EWS-FLI1 utilizes divergent chromatin remodeling mechanisms to directly activate or repress enhancer elements in Ewing sarcoma. *Cancer Cell, 26*(5), 668-681. doi:10.1016/j.ccell.2014.10.004

Riggi, N., & Stamenkovic, I. (2007). The Biology of Ewing sarcoma. *Cancer Lett, 254*(1), 1-10. doi:10.1016/j.canlet.2006.12.009

S. Burdach, Division of Pediatric Hematology/Oncology and Children's Cancer Research Center, Martin-Luther-University Halle Wittenberg, Halle, Germany, & H. Jürgens, Department of Pediatric Hematology/Oncology, Westfälische Wilhelms-University, Münster, Germany. (2000). High-dose chemoradiotherapy (HDC) in the Ewing family of tumors (EFT). *Critical Reviews in Oncology/Hematology, 41 (2002) 169–189*.

Sakimura, R., Tanaka, K., Nakatani, F., Matsunobu, T., Li, X., Hanada, M., Okada, T., Nakamura, T., Matsumoto, Y., & Iwamoto, Y. (2005). Antitumor effects of histone deacetylase inhibitor on Ewing's family tumors. *Int J Cancer, 116*(5), 784-792. doi:10.1002/ijc.21069

Sanchez, R., & Zhou, M. M. (2009). The role of human bromodomains in chromatin biology and gene transcription. *Curr Opin Drug Discov Devel, 12*(5), 659-665.

Schlottmann, S., Erkizan, H. V., Barber-Rotenberg, J. S., Knights, C., Cheema, A., Uren, A., Avantaggiati, M. L., & Toretsky, J. A. (2012). Acetylation Increases EWS-FLI1 DNA Binding and Transcriptional Activity. *Front Oncol, 2*, 107. doi:10.3389/fonc.2012.00107

Shang, E., Cui, Q., Wang, X., Beseler, C., Greenberg, D. A., & Wolgemuth, D. J. (2011). The bromodomain-containing gene BRD2 is regulated at transcription, splicing, and translation levels. *J Cell Biochem, 112*(10), 2784-2793. doi:10.1002/jcb.23192

Shang, E., Salazar, G., Crowley, T. E., Wang, X., Lopez, R. A., Wang, X., & Wolgemuth, D. J. (2004). Identification of unique, differentiation stage-specific patterns of expression of the bromodomain-containing genes Brd2, Brd3, Brd4, and Brdt in the mouse testis. *Gene Expr Patterns, 4*(5), 513-519. doi:10.1016/j.modgep.2004.03.002

Shang, E., Wang, X., Wen, D., Greenberg, D. A., & Wolgemuth, D. J. (2009). Double bromodomain-containing gene Brd2 is essential for embryonic development in mouse. *Dev Dyn, 238*(4), 908-917. doi:10.1002/dvdy.21911

Shao, Z., Zhang, R., Khodadadi-Jamayran, A., Chen, B., Crowley, M. R., Festok, M. A., Crossman, D. K., Townes, T. M., & Hu, K. (2016). The acetyllysine reader BRD3R promotes human nuclear reprogramming and regulates mitosis. *Nat Commun, 7*, 10869. doi:10.1038/ncomms10869

Shi, Junwei, & Vakoc, Christopher R. The Mechanisms behind the Therapeutic Activity of BET Bromodomain Inhibition. *Molecular Cell, 54*(5), 728-736. doi:10.1016/j.molcel.2014.05.016

Shu, S., Lin, C. Y., He, H. H., Witwicki, R. M., Tabassum, D. P., Roberts, J. M., Janiszewska, M., Huh, S. J., Liang, Y., Ryan, J., Doherty, E., Mohammed, H., Guo, H., Stover, D. G., Ekram, M. B., Brown, J., D'Santos, C., Krop, I. E., Dillon, D., McKeown, M., Ott, C., Qi, J., Ni, M., Rao, P. K., Duarte, M., Wu, S. Y., Chiang, C. M., Anders, L., Young, R. A., Winer, E., Letai, A., Barry, W. T., Carroll, J. S., Long, H., Brown, M., Liu, X. S., Meyer, C. A., Bradner, J. E., & Polyak, K. (2016). Response and resistance to BET bromodomain inhibitors in triple-negative breast cancer. *Nature, 529*(7586), 413-417. doi:10.1038/nature16508

Sun, X. X., Ma, L. M., & Wang, T. (2016). [Effect of BRD4 Inhibitor JQ1 on Proliferation Inhibition and Apotosis Induction in Jurkat Cells]. *Zhongguo Shi Yan Xue Ye Xue Za Zhi, 24*(4), 1019-1023. doi:10.7534/j.issn.1009-2137.2016.04.011

Suva, M. L., Riggi, N., Stehle, J. C., Baumer, K., Tercier, S., Joseph, J. M., Suva, D., Clement, V., Provero, P., Cironi, L., Osterheld, M. C., Guillou, L., & Stamenkovic, I. (2009). Identification of cancer stem cells in Ewing's sarcoma. *Cancer Res, 69*(5), 1776-1781. doi:10.1158/0008-5472.CAN-08-2242

Taniguchi, Y. (2016). The Bromodomain and Extra-Terminal Domain (BET) Family: Functional Anatomy of BET Paralogous Proteins. *Int J Mol Sci, 17*(11). doi:10.3390/ijms17111849

Tanner, J. M., Bensard, C., Wei, P., Krah, N. M., Schell, J. C., Gardiner, J. D., Schiffman, J. D., Lessnick, S. L., & Rutter, J. (2017). EWS/FLI is a Master Regulator of Metabolic Reprogramming in Ewing Sarcoma. *Mol Cancer Res*. doi:10.1158/1541-7786.MCR-17-0182

Taverna, Sean D., Li, Haitao, Ruthenburg, Alexander J., Allis, C. David, & Patel, Dinshaw J. (2007). How chromatin-binding modules interpret histone modifications: lessons from professional pocket pickers. *Nat Struct Mol Biol, 14*(11), 1025-1040. doi:http://www.nature.com/nsmb/journal/v14/n11/suppinfo/nsmb1338_S1.html

Thiel, U., Schober, S. J., Einspieler, I., Kirschner, A., Thiede, M., Schirmer, D., Gall, K., Blaeschke, F., Schmidt, O., Jabar, S., Ranft, A., Alba Rubio, R., Dirksen, U., Grunewald, T. G. P., Sorensen, P. H., Richter, G. H. S., von Luttichau, I. T., Busch, D. H., & Burdach, S. E. G. (2017). Ewing sarcoma partial regression without GvHD by chondromodulin-I/HLA-A*02:01-specific allorestricted T cell receptor transgenic T cells. *Oncoimmunology, 6*(5), e1312239. doi:10.1080/2162402X.2017.1312239

Tirode, F., Laud-Duval, K., Prieur, A., Delorme, B., Charbord, P., & Delattre, O. (2007). Mesenchymal stem cell features of Ewing tumors. *Cancer Cell, 11*(5), 421-429. doi:10.1016/j.ccr.2007.02.027

Tomazou, E. M., Sheffield, N. C., Schmidl, C., Schuster, M., Schonegger, A., Datlinger, P., Kubicek, S., Bock, C., & Kovar, H. (2015). Epigenome mapping reveals distinct modes of gene regulation and widespread enhancer reprogramming by the oncogenic fusion protein EWS-FLI1. *Cell Rep, 10*(7), 1082-1095. doi:10.1016/j.celrep.2015.01.042

Valdes, M., Nicholas, G., Verma, S., & Asmis, T. (2017). Systemic Therapy Outcomes in Adult Patients with Ewing Sarcoma Family of Tumors. *Case Rep Oncol, 10*(2), 462-472. doi:10.1159/000475806

Verma, V., Denniston, K. A., Lin, C. J., & Lin, C. (2017). A Comparison of Pediatric vs. Adult Patients with the Ewing Sarcoma Family of Tumors. *Front Oncol, 7*, 82. doi:10.3389/fonc.2017.00082

von Heyking, K., Calzada-Wack, J., Gollner, S., Neff, F., Schmidt, O., Hensel, T., Schirmer, D., Fasan, A., Esposito, I., Muller-Tidow, C., Sorensen, P. H., Burdach, S., & Richter, G. H. (2017). The endochondral bone protein CHM1 sustains an undifferentiated, invasive phenotype, promoting lung metastasis in Ewing sarcoma. *Mol Oncol*. doi:10.1002/1878-0261.12057

Wang, L., Wu, X., Huang, P., Lv, Z., Qi, Y., Wei, X., Yang, P., & Zhang, F. (2016). JQ1, a small molecule inhibitor of BRD4, suppresses cell growth and invasion in oral squamous cell carcinoma. *Oncol Rep, 36*(4), 1989-1996. doi:10.3892/or.2016.5037

Whyte, W. A., Orlando, D. A., Hnisz, D., Abraham, B. J., Lin, C. Y., Kagey, M. H., Rahl, P. B., Lee, T. I., & Young, R. A. (2013). Master transcription factors and mediator establish super-enhancers at key cell identity genes. *Cell, 153*(2), 307-319. doi:10.1016/j.cell.2013.03.035

Yang, Z., He, N., & Zhou, Q. (2008). Brd4 recruits P-TEFb to chromosomes at late mitosis to promote G1 gene expression and cell cycle progression. *Mol Cell Biol, 28*(3), 967-976. doi:10.1128/MCB.01020-07

Yu, H., Ge, Y., Guo, L., & Huang, L. (2017). Potential approaches to the treatment of Ewing's sarcoma. *Oncotarget, 8*(3), 5523-5539. doi:10.18632/oncotarget.12566

Yun, M., Wu, J., Workman, J. L., & Li, B. (2011). Readers of histone modifications. *Cell Res, 21*(4), 564-578. doi:10.1038/cr.2011.42

Zeng, L., & Zhou, M. M. (2002). Bromodomain: an acetyl-lysine binding domain. *FEBS Lett, 513*(1), 124-128.

Zhang, P., Dong, Z., Cai, J., Zhang, C., Shen, Z., Ke, A., Gao, D., Fan, J., & Shi, G. (2015). BRD4 promotes tumor growth and epithelial-mesenchymal

transition in hepatocellular carcinoma. *Int J Immunopathol Pharmacol, 28*(1), 36-44. doi:10.1177/0394632015572070

Zhu, X., Enomoto, K., Zhao, L., Zhu, Y. J., Willingham, M. C., Meltzer, P., Qi, J., & Cheng, S. Y. (2017). Bromodomain and Extraterminal Protein Inhibitor JQ1 Suppresses Thyroid Tumor Growth in a Mouse Model. *Clin Cancer Res, 23*(2), 430-440. doi:10.1158/1078-0432.CCR-16-0914

Zuber, Johannes, Shi, Junwei, Wang, Eric, Rappaport, Amy R., Herrmann, Harald, Sison, Edward A., Magoon, Daniel, Qi, Jun, Blatt, Katharina, Wunderlich, Mark, Taylor, Meredith J., Johns, Christopher, Chicas, Agustin, Mulloy, James C., Kogan, Scott C., Brown, Patrick, Valent, Peter, Bradner, James E., Lowe, Scott W., & Vakoc, Christopher R. (2011). RNAi screen identifies Brd4 as a therapeutic target in acute myeloid leukaemia. *Nature, 478*(7370), 524-528. doi:http://www.nature.com/nature/journal/v478/n7370/abs/nature10334.html#supplementary-information